

1972

# Isothermal grain growth and ferroelectric behavior of a fully dense lanthanum doped lead zirconate-lead titanate ceramic

Richard A. Langman  
*Lehigh University*

Follow this and additional works at: <https://preserve.lehigh.edu/etd>

 Part of the [Materials Science and Engineering Commons](#)

---

## Recommended Citation

Langman, Richard A., "Isothermal grain growth and ferroelectric behavior of a fully dense lanthanum doped lead zirconate-lead titanate ceramic" (1972). *Theses and Dissertations*. 4071.  
<https://preserve.lehigh.edu/etd/4071>

This Thesis is brought to you for free and open access by Lehigh Preserve. It has been accepted for inclusion in Theses and Dissertations by an authorized administrator of Lehigh Preserve. For more information, please contact [preserve@lehigh.edu](mailto:preserve@lehigh.edu).

ISOTHERMAL GRAIN GROWTH AND FERROELECTRIC  
BEHAVIOR OF A FULLY DENSE LANTHANUM DOPED  
LEAD ZIRCONATE-LEAD TITANATE CERAMIC

by

Richard Allan Langman

A Thesis

Presented to the Graduate Committee

of Lehigh University

in Candidacy for the Degree of

Master of Science

in

Metallurgy and Materials Science

Lehigh University

1972



CERTIFICATE OF APPROVAL

This thesis is accepted and approved in partial fulfillment  
of the requirements for the degree of Master of Science.

May 11 1972  
Date

Lesley R. Butler  
Professor in Charge

G. P. Curran  
Chairman of the Department of  
Metallurgy and Materials Science

ACKNOWLEDGEMENTS

The author wishes to make the following acknowledgements:

Dr. S. R. Butler, Lehigh University, for his patience, guidance, and assistance during the experimental work and the preparation of this manuscript.

Dr. R. B. Runk, Western Electric Co., ERC, for his invaluable assistance in the formulation of the topic and critical evaluation of the manuscript.

Dr. R. E. Mistler, Western Electric Co., ERC, for his cooperation and assistance during the project.

The technical support staff of Dept. 20413, Western Electric Co., ERC, Mrs. T. G. Steele, Mr. G. E. Crosby, Mr. L. W. Trego and especially Mr. M. J. Andrejco.

Mr. R. A. Korastinsky, Lehigh University, for diligently performing the electron microscopy work.

Mr. R. E. Woods, Western Electric Co., ERC, for his assistance in the preparation of specimens for electron microscopy.

Mr. S. G. Feltham, Western Electric Co., Allentown Works, for diligently performing the scanning electron microscopy work.

The Allentown Works, especially R. L. Kaufman, R. A. Snell, and C. R. Butler, for the opportunity to attend this program.

## TABLE OF CONTENTS

	<u>Page</u>
ACKNOWLEDGEMENTS.....	iii
LIST OF TABLES.....	v
LIST OF FIGURES.....	vi
ABSTRACT.....	1
I. INTRODUCTION.....	2
II. EXPERIMENTAL PROCEDURE.....	5
1. Material Preparation.....	5
2. Powder Characterization.....	6
3. Sample Fabrication.....	9
4. Isothermal Heat Treatment.....	12
5. Measurement Techniques.....	14
III. RESULTS AND DISCUSSION.....	16
1. Pressure-Sintered Specimens.....	16
2. Isothermal Heat Treatment.....	19
3. Isothermal Grain Growth.....	25
4. Electrical and Electromechanical Properties.....	40
IV. CONCLUSIONS.....	67
APPENDIX	
I. Electrical and Electromechanical Data.....	69
REFERENCES.....	70
VITA.....	75

## LIST OF TABLES

<u>Table</u>		<u>Page</u>
I	Wet Chemical Analysis and X-ray Spectrochemical Analysis of Calcined PLZT Powder.....	7
II	Spectrographic Analysis of Calcined PLZT Powder.....	8
III	Effect of Isothermal Heat Treatment Temperature on the Percent Weight Change Resulting From PbO Activity Equilibration.....	21
IV	Results of Least-Squares Analysis for Grain Diameter Cubed Versus Time.....	29
V	Initial Electrical and Electromechanical Properties of the Pressure-Sintered Slugs.....	41
VI	Possible Paths by Which a Nominal 7/65/35 PLZT Composition Can Approach the Rhombohedral-Tetragonal Phase Boundary and the Effect of These Paths on Properties.....	65

## LIST OF FIGURES

<u>Figure</u>		<u>Page</u>
1	Hot-Press Die Assembly.....	10
2	Electron Micrograph Showing Microstructure of Pressure-Sintered PLZT, 1075°C - 16 hrs. - 6000 psi, (3,800X).....	17
3	Scanning Electron Micrograph of a Fractured PLZT Surface (10,000X).....	18
4	Scanning Electron Micrograph of a Fractured PLZT Surface Which Has Been Thermally Etched (10,000X)...	18
5	Optical Micrograph of a Polished PLZT Specimen (1300°C - 480 minutes) Showing the Presence of a Second Phase and Porosity (500X).....	24
6	Least-Squares Plot of $\log(D^3 - D_0^3)$ versus Log Time.....	28
7	Arrhenius Plot of Grain Growth Rate versus the Reciprocal of the Absolute Temperature.....	30
8	Electron Micrograph Showing the Microstructure of Pressure - Sintered PLZT (3,800X).....	33
9	Electron Micrograph Showing the Microstructure of Pressure - Sintered PLZT (3,800X).....	33
10	Electron Micrograph Showing the Microstructure of Heat Treated PLZT, 1100°C - 480 minutes (3,800X)....	34
11	Electron Micrograph Showing the Microstructure of Heat Treated PLZT, 1100°C - 1,920 minutes (3,800X)..	34
12	Electron Micrograph Showing the Microstructure of Heat Treated PLZT, 1200°C - 480 minutes (3,800X)....	35
13	Electron Micrograph Showing the Microstructure of Heat Treated PLZT, 1100°C - 6,000 minutes (3,800X)..	35
14	Electron Micrograph Showing the Microstructure of Heat Treated PLZT, 1200°C - 1,920 minutes (3,800X)..	36



## LIST OF FIGURES (cont)

<u>Figure</u>		<u>Page</u>
15	Electron Micrograph Showing the Microstructure of Heat Treated PLZT, 1200°C - 6,000 minutes (3,800X)....	36
16	Scanning Electron Micrograph of a Typical Heat Treated (1200°C - 4,320 minutes) Specimen Which Has Been Polished (5,250X).....	38
17	Scanning Electron Micrograph Showing a Typical Heat Treated Specimen (1250°C - 1,920 minutes) Which Has Been Thermally Etched (2,100X).....	39
18	Scanning Electron Micrograph Showing a Typical Heat Treated Specimen (1250°C - 1,920 minutes) Which Has Been Thermally Etched (5,250X).....	39
19	Dielectric Constant ( $K_3^T$ ) Unpoled (A) and Poled (B) as a Function of Average Grain Diameter.....	43
20	Scanning Electron Micrograph Showing the Domain Texture in a Typical Heat Treated (1200°C - 4,320 minutes) Specimen (2,100X).....	46
21	Dissipation Factor Unpoled (A) and Poled (B) as a Function of Average Grain Diameter.....	47
22	Planar Coupling Factor ( $k_p$ ) as a Function of Average Grain Diameter.....	50
23	Dielectric Constant as a Function of Temperature.....	52
24	Dielectric Constant as a Function of Temperature.....	54
25	Relative Dielectric Constant at the Curie Temperature as a Function of Average Grain Diameter...	57
26	Dissipation Factor as a Function of Temperature.....	59
27	Dissipation Factor as a Function of Temperature.....	61

## ABSTRACT

Theoretically dense PLZT ( $\text{Pb}_{.93}\text{La}_{.07}(\text{Zr}_{.65}\text{Ti}_{.35})_{.9825}\text{O}_3$ ) specimens with average grain diameters of  $\approx 1 \mu\text{m}$  were fabricated by a pressure-sintering technique. Specimens were characterized with respect to their electrical and electromechanical properties. The fully dense, single-phase specimens were isothermally heat treated in the temperature range of  $1100^\circ\text{C} - 1250^\circ\text{C}$  for various times in a low activity ( $\text{PbO}$ ) atmosphere to observe isothermal grain growth kinetics and ferroelectric property variation.

The isothermal grain growth of PLZT specimens (in the presence of the low activity atmosphere) obeys the  $D^3 - D_0^3 = k't$ , relationship with a phenomenological activation energy of  $86 \text{ K cal./mole}$ . A solid solution (impurity) drag mechanism is proposed as the controlling grain growth rate mechanism.

Most dielectric and ferroelectric properties were observed not to be a function of the average grain diameter in the range  $1-5 \mu\text{m}$ . However, the heat treated specimens displayed a 20% increase in the planar coupling factor compared to the pressure-sintered specimen values. This is thought to be due to the introduction of point defects within the single-phase PLZT specimen.

## I. INTRODUCTION

A number of interesting properties of ferroelectric ceramics in the solid solution system lead zirconate-lead titanate (PZT) have been recognized and studied for several years. The majority of the available literature (1-13) concerns itself with PZT compositions prepared by conventional sintering techniques and modified by various additions to the solid solution.

Only in recent years have investigators (14-17) concerned themselves with the properties of pressure-sintered compositions in the PZT solid solution system. Extensive studies conducted by Haertling and co-workers (18-22) on pressure-sintered PZT ceramics containing bismuth eventually led to the development of an electro-optic polycrystalline ceramic. Presently investigations by Haertling and co-workers (23-24) have been concerned with the development of an improved electro-optic material, this being a lanthanum modified lead zirconate-lead titanate (PLZT) ceramic. These modified PZT materials developed by Haertling and co-workers at Sandia Corporation exhibit electrically variable coefficients of piezoelectricity and birefringence, as well as a high degree of optical transparency in thin polished plates. Consequently, these ferroelectric ceramics are of particular interest for a variety of electro-optic device applications (22, 25-28).

The performance of the electro-optic devices depends to a considerable extent on the properties inherent to the ferroelectric



ceramic. Thus, one approach for achieving improved electro-optic devices is to fabricate the ceramic with precisely controlled ferroelectric and optical properties. The optimization of these properties can be achieved by carefully controlling the following: (1) chemical composition, (2) chemical homogeneity, (3) microstructure and (4) density (near theoretical).

The variation of the piezoelectric and ferroelectric properties of a polycrystalline material relative to its microstructure has been investigated to some extent (12, 20, 29-31). More specifically the relevant aspects of microstructure studied have been size and distribution of the grains and pores, and phase constitution. These investigations have shown that properties can be considerably altered by the variation of these microstructural parameters. Therefore, microstructural development is important if controlled and reproducible piezoelectric and ferroelectric properties are to be realized.

The present study was undertaken with the purpose of examining the influence of certain microstructural features on the electrical and electromechanical properties of PLZT ferroelectric ceramics. The text will present the results obtained for a fine-grained ( $\approx 1 \mu\text{m}$ ) pressure-sintered PLZT composition, which was isothermally heat treated in an effort to obtain specimens with a controlled microstructural variation. The nominal composition selected for this study contained seven atom percent lanthanum and a 65/35

atom ratio of Zr/Ti (designated 7/65/35)\*.

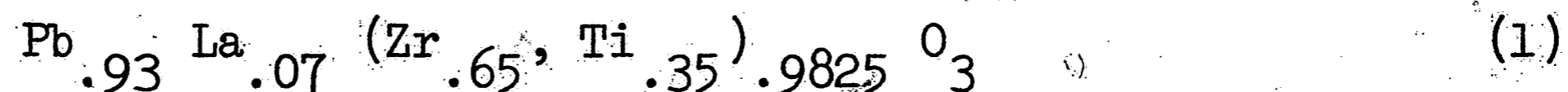
---

\*This composition is discussed in references (23, 24).

## II. EXPERIMENTAL PROCEDURE

### 1. Material Preparation

A 500 gram lanthanum doped lead zirconate-lead titanate composition was compounded from the appropriate oxides\* in accordance with the following chemical formula



The basic powder preparation procedure was a modified version of the technique employed by Haertling (24). Dry oxides of PbO, TiO<sub>2</sub> and ZrO<sub>2</sub> were weighted to the nearest 0.1 gram. La<sub>2</sub>O<sub>3</sub> was weighted hot to the nearest 0.1 gram following a heat treatment\*\* at 900°C for 1.5 hours in a clean Pt crucible in order to insure complete removal of any moisture present. The oxides were then transferred to a one quart polyethylene jar mill containing high density alumina grinding media and milled for 1 hour in a minimum amount of distilled water. The slurry was then poured into a Buchner funnel containing a filter\*\*\* paper, and a mechanical vacuum pump was utilized to remove the water.

---

\* U.H.P. PbO, Electronic grade, Hammond Lead Products, Inc., Hammond, Indiana; ZrO<sub>2</sub> C. P. Grade, Tizon Chemical Company, Flemington, New Jersey; TiO<sub>2</sub> Type 2650, Whittaker, Clark and Daniels, Inc., New York, New York; La<sub>2</sub>O<sub>3</sub>, City Chemical Corporation, New York, New York.

\*\* Heat treatment temperature was determined by a preliminary thermogravimetric analysis.

\*\*\* No. 42 Whatman Filter Paper, W & R Balston Limited, England.

The resultant filter cake was then transferred to a teflon bowl and dried at 110°C for several hours. The dried filter cake was then crushed in a teflon bowl with a teflon pestle and passed through a 65 mesh sieve prior to calcining at 900°C for 1 hour in a covered alumina crucible. The reacted material was then placed in a polyethylene jar mill containing high density alumina grinding media and milled for 1 hour in a minimum amount of acetone. This slurry was then poured into a Buchner funnel containing a filter paper, and a mechanical vacuum pump was utilized to remove the acetone. The filter cake was then transferred to a teflon bowl and dried at 110°C for several hours. The dried filter cake was then crushed in a teflon bowl with a teflon pestle and passed through a 65 mesh sieve prior to heat treating at 700°C for 30 minutes in a covered alumina crucible. This heat treatment was employed to remove any residual acetone which would result in a chemical reduction of the PLZT slug upon pressure-sintering. The heat treated powder was then forced through a 400 mesh nylon sieve using a teflon pestle.

## 2. Powder Characterization

Quantitative chemical analysis determinations for the four major elemental components of the calcined PLZT powder are reported in Table I in weight percent oxide. A duplicate analysis was also performed in order to ascertain the relative accuracy of the chemical analysis. The determination of lanthanum by this



TABLE I  
 WET CHEMICAL ANALYSIS\* AND X-RAY SPECTROCHEMICAL\*\*  
 ANALYSIS OF CALCINED PLZT POWDER

Oxide	Theoretical Composition	Wet Chemical		X-Ray
	Wt. %	1st analysis Wt. %	2nd analysis Wt. %	Spectrochemical Wt. %
La <sub>2</sub> O <sub>3</sub>	3.51	4.00	3.71	3.22
PbO	63.84	63.74	64.30	66.11
ZrO <sub>2</sub>	24.20	23.73	23.64	22.81
TiO <sub>2</sub>	8.45	8.44	8.41	7.86

\* National Spectrographic Laboratories, Inc.,  
 19500 South Miles Road, Cleveland, Ohio

\*\* Ms. S. M. Vincent, Bell Laboratories  
 Murray Hill, New Jersey

TABLE II  
SPECTROGRAPHIC ANALYSIS\* OF CALCINED PLZT  
POWDER

<u>Element</u>	<u>Weight Percent Oxide</u>
Al	0.051
Si	0.044
Ca	0.013
K	0.005
Fe	0.003
Mg	0.003
Ag	<0.001
Cu	<0.001
Mn	<0.001
Ba	<0.001
Na	<0.001

\* National Spectrographic Laboratories, Inc.,  
19500 South Miles Road, Cleveland, Ohio

technique, as indicated in Table I, displays the greatest degree of variation, while zirconium, lead, and titanium determinations were shown to be more repeatable. X-ray spectrochemical analysis, as reported in Table I, was utilized in order to further characterize the chemical composition of the calcined powder. In the opinion of the analyst the values determined for lead and zirconium by this technique are susceptible to the greatest degree of error.

Spectrographic analysis for the determination of the impurities present in the calcined powder are given in Table II. Based upon raw material specifications the two major impurities ( $\text{Al}_2\text{O}_3$  and  $\text{SiO}_2$ ) present are attributable to the zirconium dioxide. The two milling operations employing high alumina grinding media also contribute to the  $\text{Al}_2\text{O}_3$  impurity level detected.

### 3. Sample Fabrication

Specimens were dry-pressed at 3000 psi into a slug 0.875 inches in diameter and approximately 1.1 inches high. The specimen slug was then placed in the vacuum hot-press\* assembly (Figure 1) and the chamber was pumped down to approximately  $1 \times 10^{-5}$  torr for the 24 hours prior to the pressure-sintering of the slug. Just prior to the actual pressure-sintering of the slug the chamber was backfilled to a pressure of approximately 19.7 psi

---

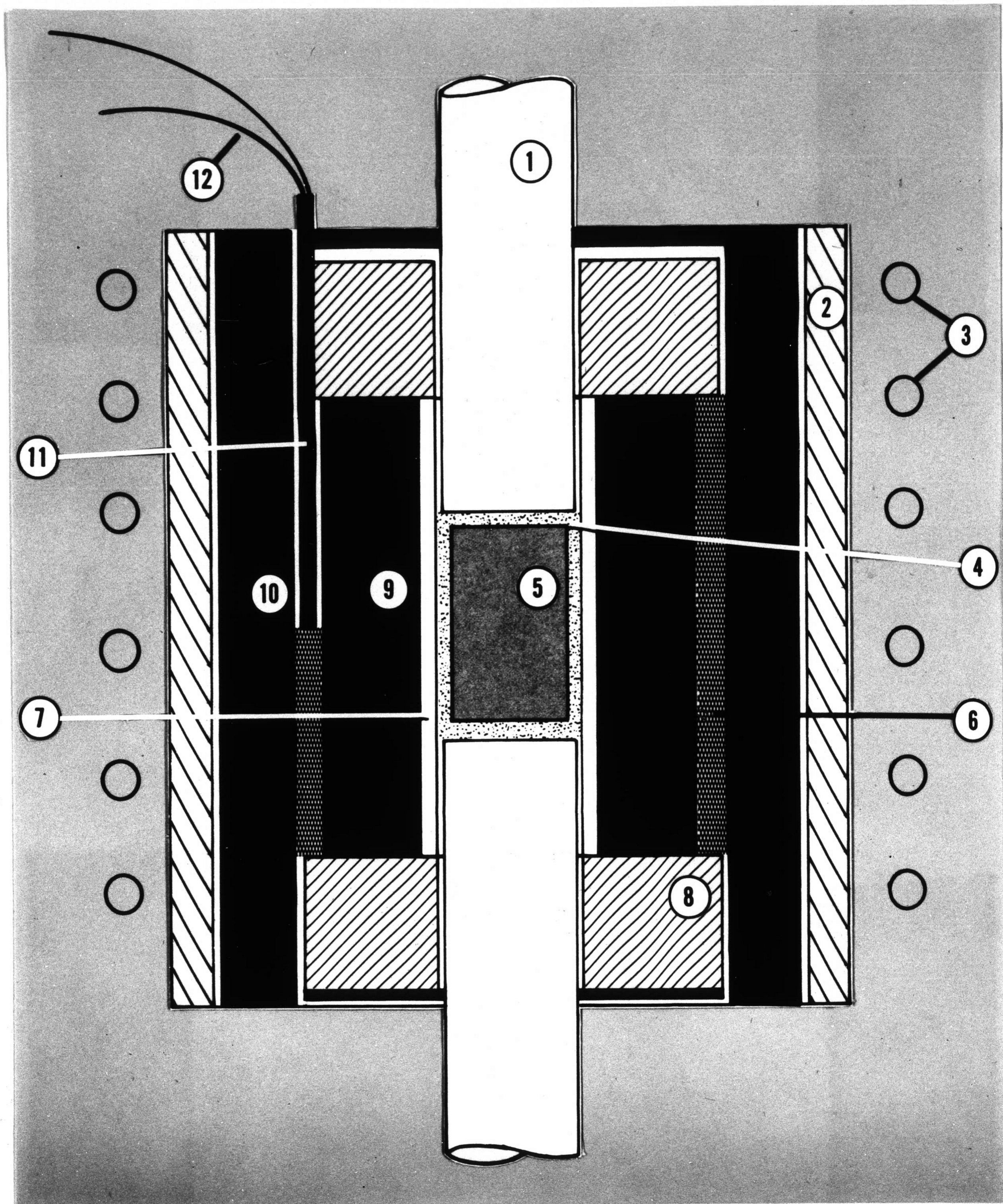
\* Vacuum Hot-Press Sintering Furnace, Series 3600, Model 1-2300, Vacuum Industries, Inc., Somerville, Massachusetts.

FIGURE 1  
HOT-PRESS DIE ASSEMBLY

LEGEND

1. UPPER ALUMINA PLUNGER
2. FUSED - SILICA INSULATION SLEEVE
3. INDUCTION COIL
4. > 60 MESH ZIRCONIA PACKING POWDER
5. PLZT SLUG
6. ZIRCONIA - FELT INSULATION LINING
7. ALUMINA DIE SLEEVE
8. CASTABLE CERAMIC INSULATION
9. SILICON CARBIDE SLEEVE
10. HASTELLOY X SUSCEPTOR
11. Pt TO Pt-13% Rh THERMOCOUPLE
12. THERMOCOUPLE LEADS







with a gas mixture consisting of 80% He - 20% O<sub>2</sub>. The Hastelloy X susceptor was then inductively heated at the average rate of 540°C per hour. A pressure of 6000 psi was applied to the slug 30 minutes after temperature stabilization was achieved at 1075°C. The slugs were pressure-sintered for a total of 16 hours with the pressure being maintained at 6000 ± 200 psi during the first 5 hours and 6000 ± 500 psi during the remaining time. At the end of the 16 hour period the pressure was removed while the sample was at temperature and the R. F. power to the susceptor was gradually reduced over a 1 hour period. The pressure-sintering conditions used, i.e., time, temperature, pressure, atmosphere, and sample size were determined by a preliminary study to yield slugs of maximum bulk density consistent with a fine grain size. Upon removal of the slug from the hot-press assembly its bulk density was determined using the Archimedes' liquid displacement technique. The slug was then machined\* to a diameter of 0.500 inches and sliced to produce disks 0.030 inches thick.

#### 4. Isothermal Heat Treatment

Two disks from each pressure-sintered slug were retained in order to characterize the initial properties of a given slug. These disks were selected such that one disk came from the center of the slug, while the other originated at the end of the slug. Also, one disk was selected at random and broken into quarters to facili-

---

\* Insaco Incorporated, P. O. Box 422, Quakertown, Pennsylvania 19851.

tate grain diameter determinations at the various times for a given temperature. Prior to isothermal heat treatment of the PLZT disks, from which electrical property measurements were determined, their weights were carefully determined and recorded.

Closed end Pt tubes approximately 5 inches in length by 0.65 inches in diameter were fabricated and loaded with a two phase mixture consisting of 15 grams of 90 weight %  $\text{PbZrO}_3$  - 10 weight %  $\text{ZrO}_2$  in order to provide a PbO atmosphere of constant activity during the isothermal heat treatment. Each individual disk and an accompanying quarter disk were vertically positioned in the packing powder and then the Pt vessel was welded shut. The Pt vessels containing the PLZT disks of a given slug were then placed in a Pt wound tube furnace and heated up to the appropriate temperature of interest at the rate of  $200^\circ\text{C}$  per hour. Pt vessels containing disks which were heat treated for relatively short periods of time (< 8 hours) were positioned in the hot zone of the tube furnace while the furnace was at the temperature of interest. In all instances the Pt vessels were removed at temperature upon attainment of the desired soak period and then immediately placed in a furnace at  $600^\circ\text{C}$  and allowed to furnace cool to room temperature. Once at room temperature the samples were removed from the Pt vessel, the packing powder was removed from the disk, and the weight of the heat treated disk determined and recorded.

## 5. Measurement Techniques

Specimens for grain diameter determinations were mechanically polished on 600 grit SiC paper and then on a Syntron bowl containing a slurry of 0.3  $\mu\text{m}$  gamma alumina powder. These specimens were then thermally etched for 20 minutes at  $1050 \pm 50^\circ\text{C}$  in a covered Pt crucible containing a mixture of 90 weight %  $\text{PbZrO}_3$  - 10 weight %  $\text{ZrO}_2$  powder in order to provide a PbO rich atmosphere. Formvar two-stage replicas were then prepared of the thermally etched surface for examination in the electron microscope. Average grain diameter measurements were determined from electron microscope photomicrographs by the linear intercept method as described by Hillard (32). The average equivalent spherical grain diameter was then determined by multiplying the average intercept length by 1.5 as suggested by Fullman (33). The coefficient of variation of the average intercept length was maintained at less than 7 percent by counting a minimum of at least 80 intersections. Wherever possible the accuracy of the technique was improved by counting approximately 200 intersections.

Ferroelectric domain texture was revealed by chemically etching polished specimens with a dilute (5%) solution of HCl in distilled water containing 1 drop of 50% HF per 100  $\text{cm}^3$  of solution. These specimens were then evaporated with gold and examined in a scanning electron microscope.

Electrical property measurements were made on PLZT disks which were electroded by evaporating titanium and then gold on the disks major surfaces. Several days after electroding electrical property measurements were performed on the disks just prior to poling and 24 hours after poling. The disks were poled at room temperature in a freon bath with an applied electric field of 20 kV/cm maintained for 5 minutes.

A capacitance bridge\* was utilized for small signal dielectric measurements of capacitance and dissipation factor ( $\tan \delta$ ) at 1 kHz. Determinations of the planar coupling factor ( $k_p$ ) were made by the resonance - antiresonance technique in accordance with the IRE Standards on piezoelectric ceramics (34).

---

\*Type 1673-A Automatic Capacitance Bridge and Type 1672-AS2 Digital Control Unit, General Radio Company, Concord, Massachusetts



### III. RESULTS AND DISCUSSION

#### 1. Pressure-Sintered Specimens

Pressure-sintered slugs were reproducibly fabricated with bulk densities of  $7.855 \pm 0.000$  gm/cm<sup>3</sup> and average grain sizes of  $1.1 \pm 0.2$   $\mu$ m. The theoretical density for the 7/65/35 composition has been reported by Haertling and Land (23) to be 7.856 gm/cm<sup>3</sup>. This indicates the fabrication procedure has yielded slugs with very high relative densities. Average grain size determinations indicated that grain size gradients within a given slug were very small ( $\leq 0.05$   $\mu$ m).

The microstructural character of a typical pressure-sintered slug is shown in Fig. 2. The electron micrograph of the polished and thermally etched specimen clearly depicts a highly dense material consisting of relatively uniform equiaxed grains. Additional microstructural examination was performed on the surface produced by fracturing a specimen. The scanning electron micrograph, shown in Fig. 3, clearly illustrates the intercrystalline nature of the fracture. The effect of thermally etching the same specimen as described in section II-5 is shown in Fig. 4. The scanning electron micrograph shows the rather rapid rounding of the fractured surface grains to lower the energy configuration. No strong surface energy anisotropy effects are in evidence. This rapid transition of the surface grains under thermal etching conditions is thought to be aided by the high vapor transport rate of PbO at the surface of the

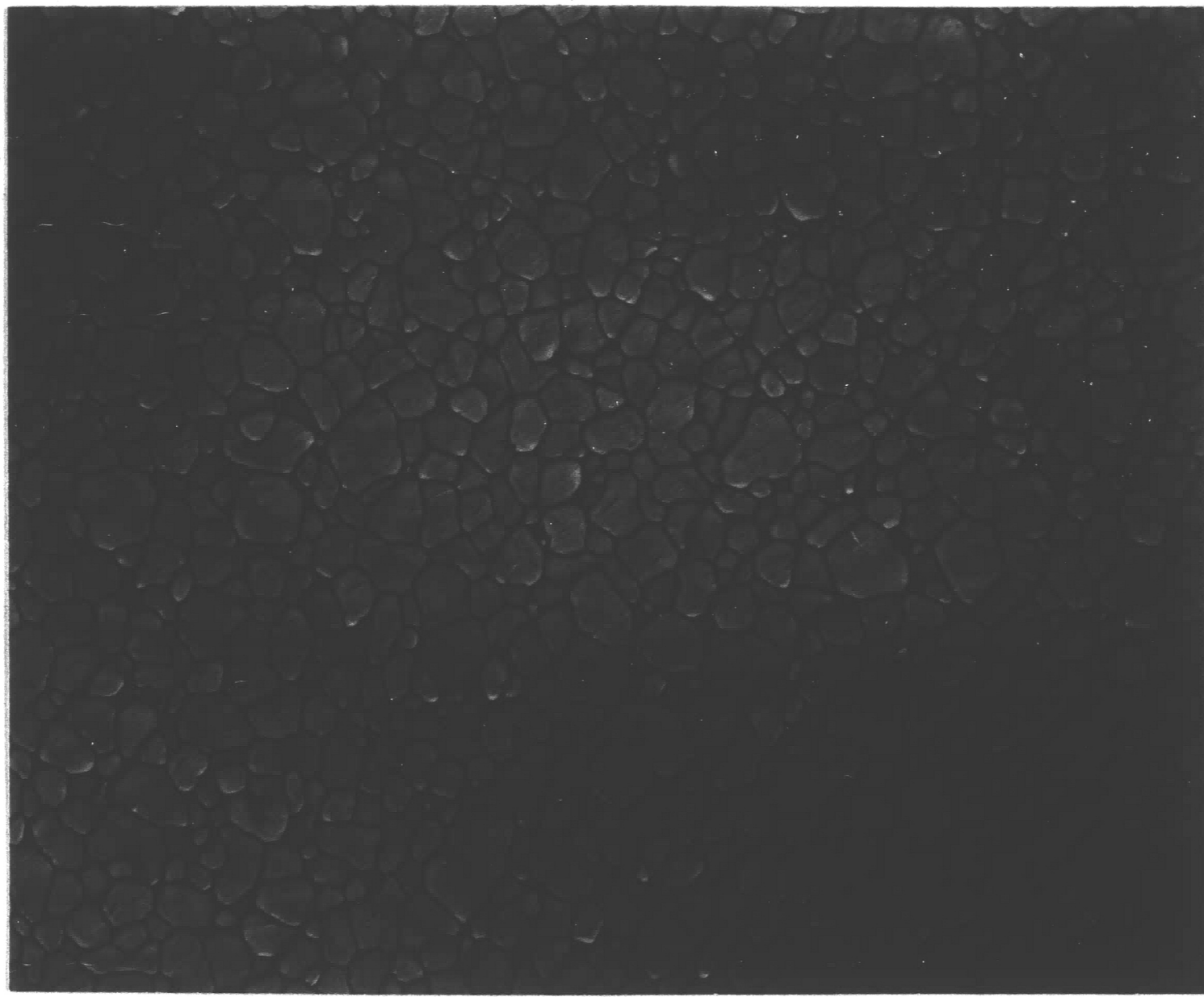


FIGURE 2  
ELECTRON MICROGRAPH SHOWING MICROSTRUCTURE OF  
PRESSURE-SINTERED PLZT, 1075°C-  
16 HRS. - 6,000 PSI, (3,800X)



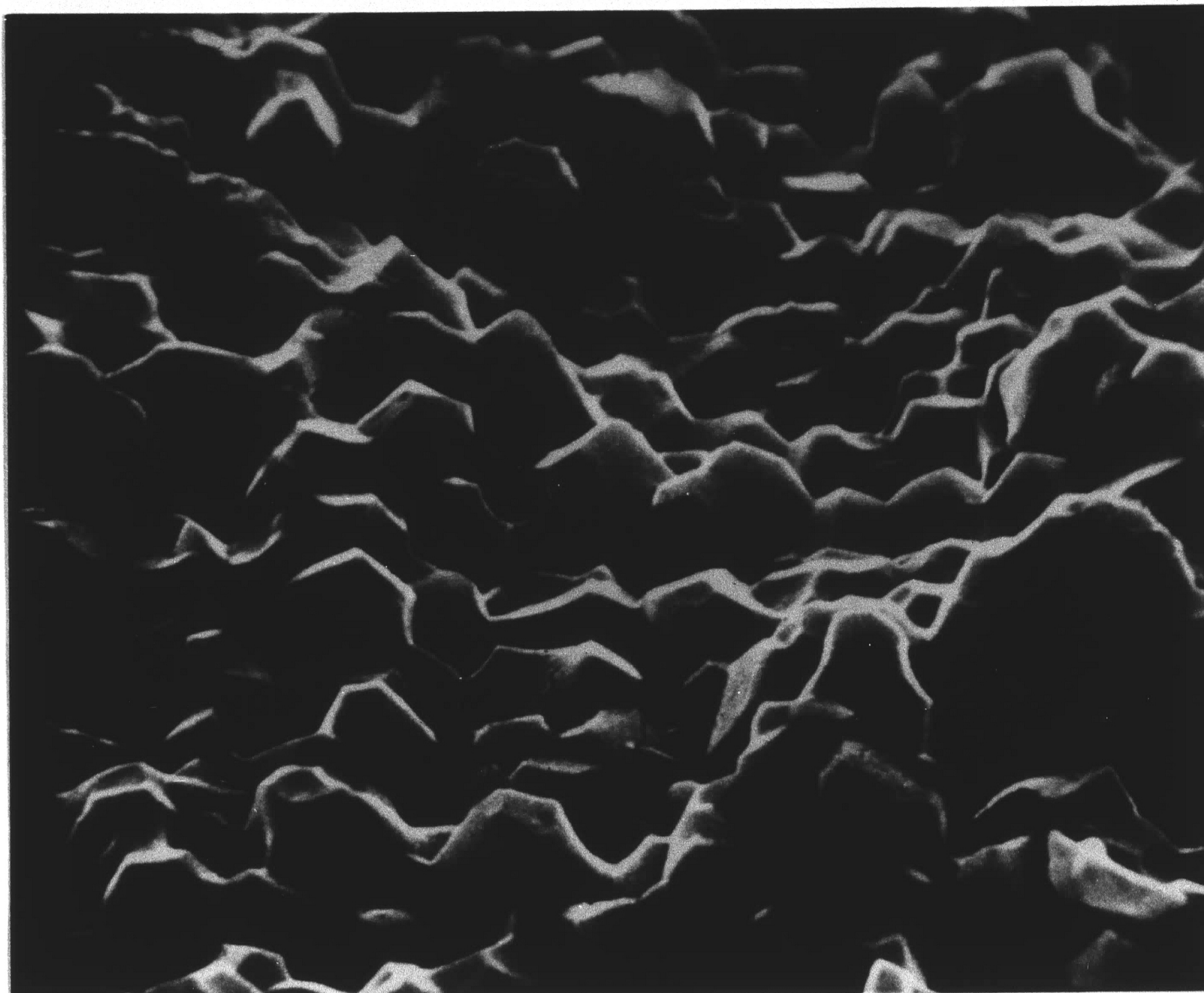


FIGURE 3  
SCANNING ELECTRON MICROGRAPH OF A  
FRACTURED PLZT SURFACE (10,000X)



FIGURE 4  
SCANNING ELECTRON MICROGRAPH OF A FRACTURED PLZT SURFACE  
WHICH HAS BEEN THERMALLY ETCHED (10,000X)



specimen. The Zr, Ti, and La ions present at the surface must also move rapidly by volume or surface diffusion which is enhanced by the vapor transport of PbO.

## 2. Isothermal Heat Treatment

In the temperature region studied (1100°C - 1300°C) the PLZT material contains two species which are quite volatile, these being PbO and O. The mechanism and kinetics of PbO loss in PZT ceramics has been investigated by Northrop (35, 36). Atkin and Fulrath (9) have established that single-phase PZT can exist over a range of stoichiometries by accommodating changes in the concentration of lattice vacancies. However, an equilibrium atmosphere of sufficient PbO activity must be provided in order to maintain the PZT composition in the single-phase field with a constant Zr/Ti ratio. In the present study this was accomplished by the use of the 90 weight %  $\text{PbZrO}_3$  - 10 weight %  $\text{ZrO}_2$  mixture. Such a two phase mixture in a binary system will have a constant activity. According to the data of Atkin and Fulrath (9) the PbO activity will be about 0.05. Since activities decrease upon substitution of Ti for Zr (9) we are assured our 65/35 composition will be within the single-phase field. How near the boundary (saturated with  $(\text{Zr, Ti})\text{O}_2$ ) and what effect 7 atom percent lanthanum substitution will have are unknown.

Lead zirconate - lead titanate possesses the perovskite crystal structure with the Pb ions on the A sites, the corners, the Ti or Zr ions on the B sites, the center, and O ions on the faces of the unit cell. Substantial lattice vacancies may be introduced into the

perovskite structure if the electroneutrality requirement is satisfied. Suggested mechanisms which may operate to satisfy this requirement include an anion vacancy formation at an adjacent lattice site, substitution of an ion on an adjacent site with an incorrect valence, or the localization of electron holes at the vacancy.

In PLZT vacancies are introduced by the random substitution of  $\text{La}^{+3}$  on  $\text{Pb}^{+2}$  sites producing (A site) vacancies and probably a smaller fraction of  $\text{Zr}^{+4}$  and  $\text{Ti}^{+4}$  (B site) vacancies. During the heat treatment of the PLZT the formation of Pb and O vacancies occur whose concentrations are controlled by the PbO activity of the system.

As anticipated an activity equilibration process was observed to take place between the two phase ( $\text{PbZrO}_3$  and  $\text{ZrO}_2$ ) packing powder and the PLZT disk. The PLZT disks in all cases lost weight, presumed to be PbO, as a result of this process. These weight losses as determined from the disks percent weight change were observed to be temperature dependent and are given in Table III. This observed temperature dependence corresponds to an increasing relative difference between the PbO activity of the disk and the packing powder with temperature. The activity equilibration process as monitored by the disks weight change was approximately 60 percent complete within the first half hour and fully complete in less than three hours. Therefore, for the majority of the time at temperature during the heat treatment the samples were at equilibrium.

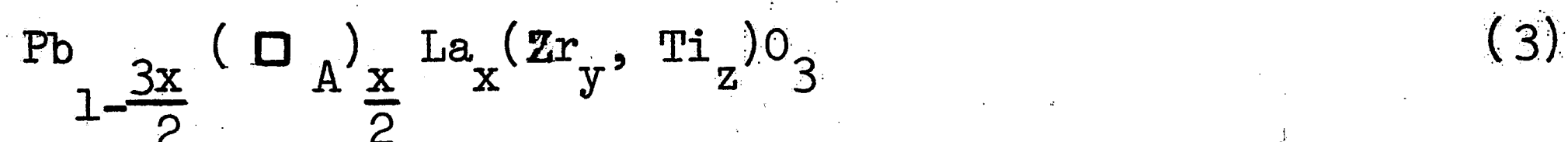
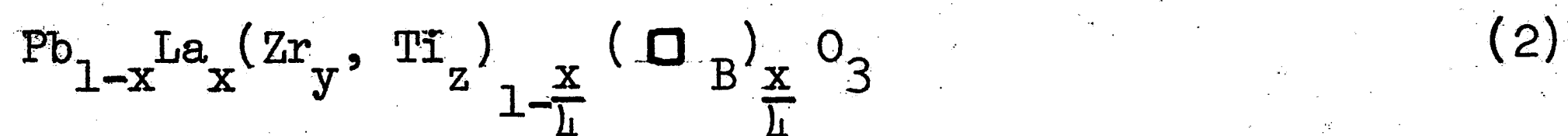
Haertling and co-workers (23) have similarly observed PbO losses to take place during conventional sintering studies of PLZT in

TABLE III

Effect of Isothermal Heat Treatment Temperature On  
The Percent Weight Change Resulting From PbO Activity Equilibration

<u>Temperature °C</u>	<u>Range of Heat Treating Times (Minutes)</u>	<u>Percent Weight Change</u>
1100	480 - 11,820	- 1.16 ± 0.21
1150	480 - 6,500	- 1.64 ± 0.04
1200	180 - 6,120	- 1.79 ± 0.17
1250	180 - 1,920	- 2.48 ± 0.07
1300	480 - 1,920	- 4.89 ± 0.49

a PbO rich atmosphere. The investigation utilized samples based on the same formula composition used in the present study (see eq. 2) and an alternate formula composition (see eq. 3) commonly used for PZT preparation with three-valent dopants such as lanthanum.



Specimens whose composition were based on equation 2 consistently lost PbO to the atmosphere, while those based on equation 3 consistently gained PbO. Since Haertling does not provide the exact experimental details, i.e., activity of the PbO atmosphere, composition studied, and sintering temperature, a precise comparison with the present study can not be made. However, the present study does indicate that equation 2 is probably PbO rich with respect to the activity given by the  $\text{PbZrO}_3 - \text{ZrO}_2$  packing powder.

The samples which experienced weight losses of less than approximately 2.6 weight percent (see Table III) retained their characteristic yellow appearance and were transparent to light in thin polished plates. Examination of the polished disks by means of the light microscope did not reveal the presence of a second phase. Therefore, these disks were still considered to be in the single-phase field, but of modified stoichiometry depending upon their weight losses.



PLZT specimens which experienced weight losses in excess of 2.6 weight percent were brownish in appearance, as opposed to their initial yellow appearance. Optical microscopy as performed on these polished specimens revealed the presence of an apparent second phase (see Fig. 5) and also the introduction of a considerable amount of porosity.

The precipitation of a second phase in PZT ceramics has been explained (12, 37) on the basis that excessive PbO losses produce a shift in the Zr/Ti atom ratio. Therefore, PbO losses which can not be fully accommodated by lattice vacancies results in a compositional shift towards a material of a lower zirconium atom ratio and the subsequent precipitation of  $ZrO_2$  as a second phase. This process is consistent with the activity composition relationship displayed by the data of reference 9.

Weight losses in excess of 2.6 weight percent (values as high as 5.6 weight percent were observed) were observed to occur under the following heat treating conditions (1) greater than 180-480 minutes at  $1300^\circ C$  (2) greater than 1950 minutes at  $1250^\circ C$  and (3) greater than 6120 minutes at  $1200^\circ C$ . The observed weight losses under the conditions cited did not vary in any consistent manner with time or temperature. Although the exact mechanism producing these excessive weight losses was not investigated, possible explanations are: (1) diffusion of PbO into the Pt vessel and (2) poor sealing of the Pt vessel allowing PbO vapor to escape. In any



FIGURE 5

OPTICAL MICROGRAPH OF A POLISHED PLZT SPECIMEN (1300°C-480 MINUTES)  
SHOWING THE PRESENCE OF A SECOND PHASE AND POROSITY (500X)

event these two-phase samples were excluded from consideration in the grain growth study reported next.

### 3. Isothermal Grain Growth

Virtually no information is available in the literature concerning the isothermal grain growth of fully dense PZT or modified PZT ceramic systems. Generally the previous grain growth studies (9, 18) have been conducted with a varying degree of complication due to the simultaneous densification process, chemical homogenization and the presence of porosity. In the present study an attempt was made to eliminate these variables and investigate the isothermal grain growth kinetics of a fully dense fine-grained lanthanum modified PZT ceramic.

During heat treatment at elevated temperatures of a fine-grained polycrystalline material an increase in the average grain diameter is observed. This increase in grain diameter results from the decrease in energy achieved by means of decreasing the grain boundary area and thus the total boundary energy of the sample.

When the grain boundary mobility is the controlling parameter for grain growth, the rate should be inversely proportional to the average radius of curvature of the boundary (38, 39). This boundary curvature is then taken to be inversely proportional to the average grain diameter. Thus, equation 4 gives the grain diameter-time



relationship obtained for the situation where the boundary mobility is rate controlling.

$$D^2 - D_0^2 = kt \quad (4)$$

The instantaneous average grain diameter is given by  $D$  and it is equal to  $D_0$  when the time equals zero. The grain growth rate constant  $k$  depends upon the temperature and the mobility of the boundary.

It has been commonly observed that the mobility of the grain boundary can be drastically altered such that the grain growth rate becomes proportional to the cube root of time (40-42). Brook (43) has summarized the particular processes which produce the cubic relationship as follows: (a) coalescence of a second phase (44) by lattice diffusion (45), (b) coalescence of the grains in the presence of a liquid phase by a solution - precipitation mechanism (46), (c) boundary migration impeded by a solid solution (impurity) drag mechanism (47) and (d) pore drag mechanisms. The equation describing the grain growth relation for these rate controlling mechanisms is given in equation 5.

$$D^3 - D_0^3 = k't \quad (5)$$

As pointed out previously the experimental data utilized in order to ascertain the controlling grain growth relation (see eq. 4 and 5) was obtained from specimens which were still single-phase and hence had weight losses of 2.6 weight percent or less. The grain



growth rate observed in these specimens was also considered to be independent of any Pb or O activity variations (9).

The best fit to the isothermal grain growth data, as shown in Fig. 6, was obtained with equation 5 rather than equation 4. A period of incubation or induction for grain growth is suggested in Fig. 6 at the lowest temperature and shortest time, therefore, this data point was not considered in the determination of the least-squares line. Grain growth rate constants and correlation coefficients resulting from a least-squares fit, for each temperature studied, are presented in Table IV. The correlation coefficients obtained from fitting the quadratic relation (equation 4) to the data were also determined and are given in Table IV. In all instances the best fit to the isothermal grain growth data, as indicated by the higher correlation coefficients, occurred with equation 5.

A phenomenological "activation energy," as determined by a least-squares analysis of the grain growth rate constants ( $k'$ ) given in Table IV, was 86 K cal./mole. An Arrhenius type plot of the grain growth rate versus the reciprocal of the absolute temperature is given in Fig. 7.

The observation of the  $t^{1/3}$  dependence of the average grain diameter in the present study is thought to be due to a solid solution (impurity) drag mechanism as proposed by Brook (47). The

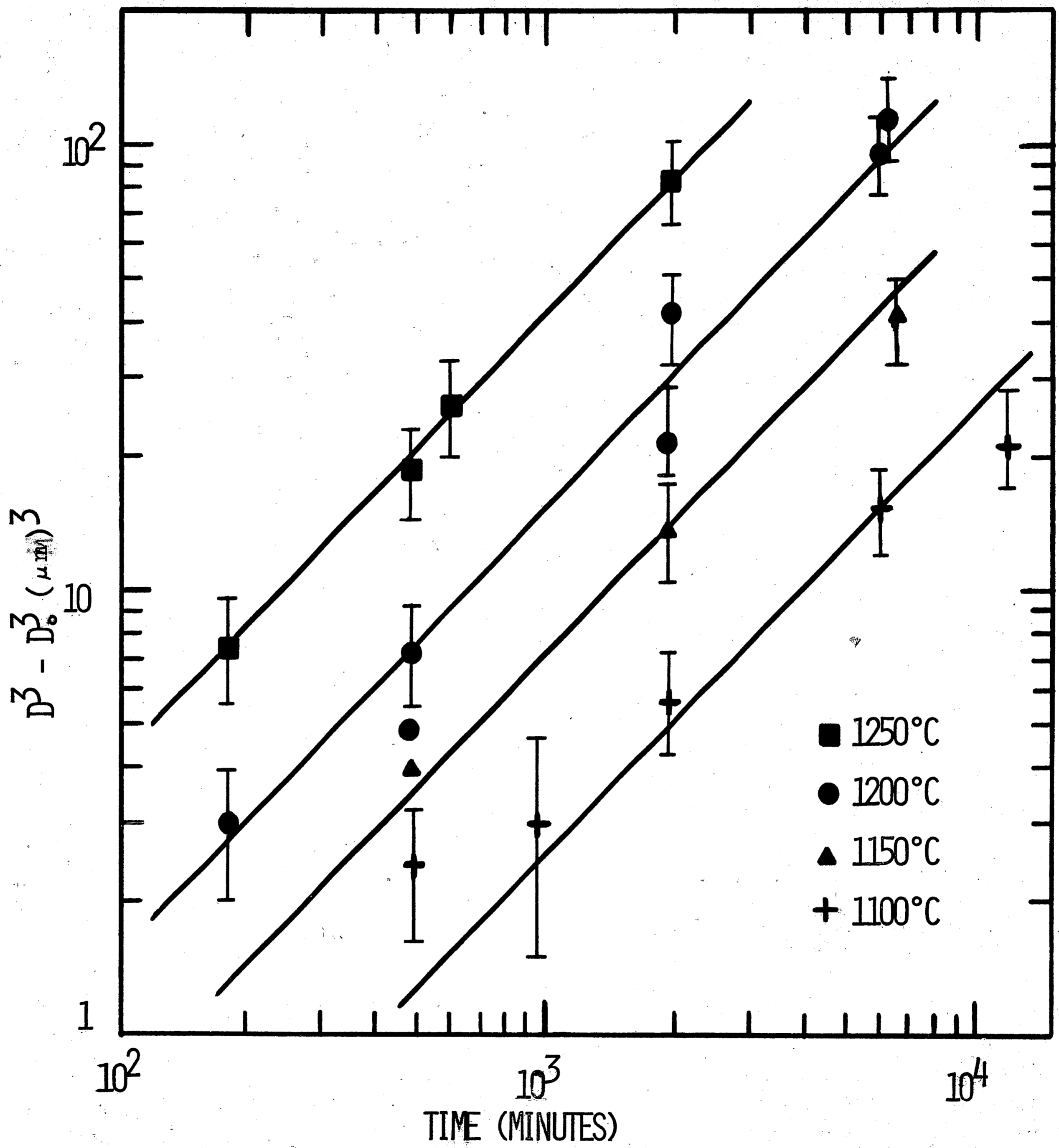


FIGURE 6  
LEAST-SQUARES PLOT OF  $\text{LOG}(D^3 - D_0^3)$  VERSUS  $\text{LOG TIME}$

TABLE IV

RESULTS OF LEAST-SQUARES ANALYSIS FOR  
GRAIN DIAMETER CUBED VERSUS TIME

<u>Temperature °C</u>	<u>k' cm<sup>3</sup>/sec</u>	<u>Correlation Coefficient*</u>
1100	$3.25 \times 10^{-17}$	0.9907
1150	$1.04 \times 10^{-16}$	0.9992
1200	$2.94 \times 10^{-16}$	0.9893
1250	$7.16 \times 10^{-16}$	0.9989

\*Correlation coefficients determined for grain diameter squared versus time from 1100°C to 1250°C respectively were 0.9669, 0.9866, 0.9853, and 0.9886.



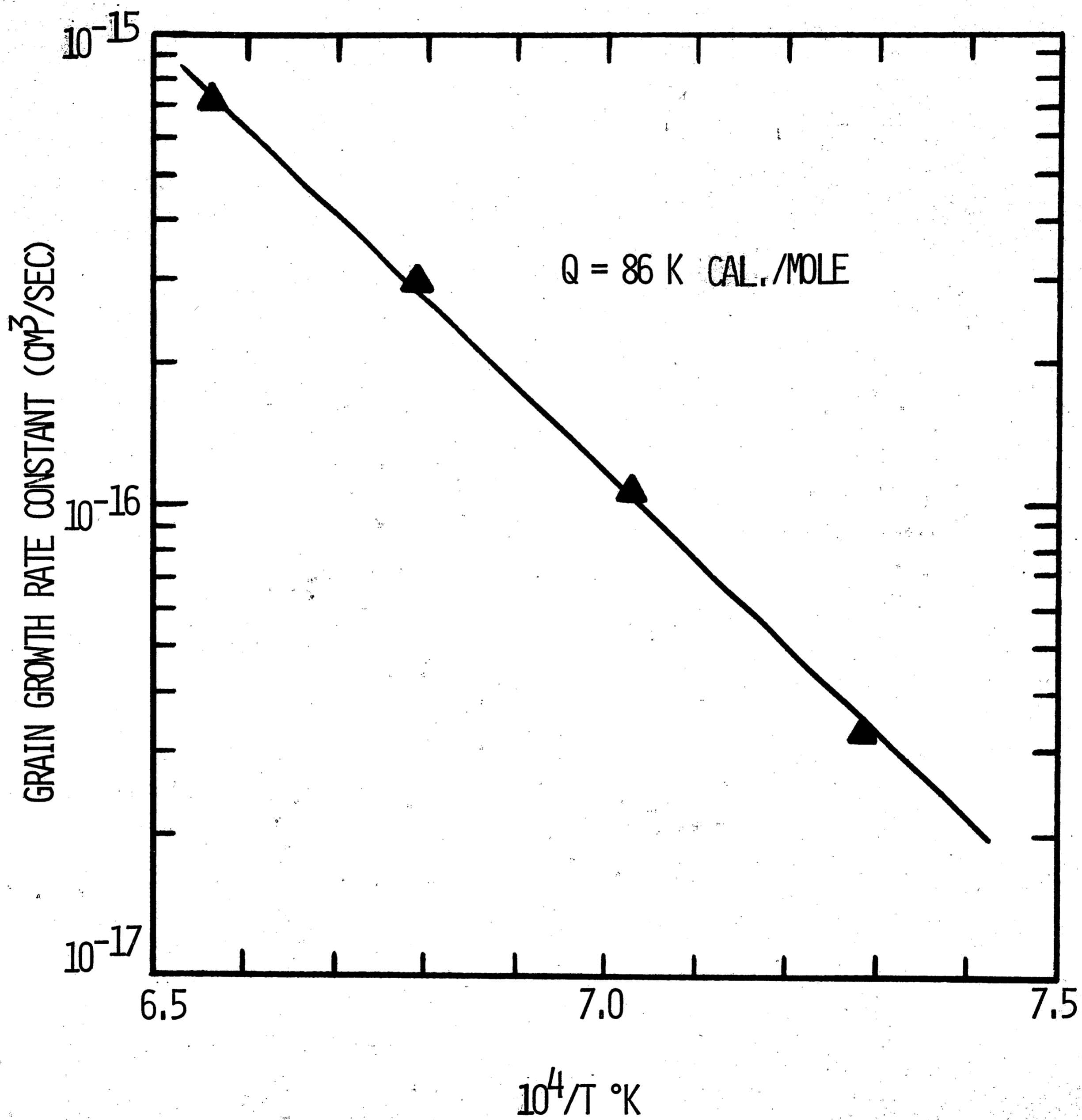


FIGURE 7

ARRHENIUS PLOT OF GRAIN GROWTH RATE VERSUS THE RECIPROCAL OF THE ABSOLUTE TEMPERATURE

other possible mechanisms as previously discussed were discounted based upon the following: (a) the presence of a second phase was not detected, (b) equilibration with the low activity atmosphere occurred over a relatively short period of time and upon attainment of this equilibrium condition, a Pb rich liquid should not be present, and (c) essentially fully dense PLZT specimens were utilized in this study.

The process by which a solid solution (impurity) drag mechanism becomes operative in PZT systems may be related to the presence of doping ions (9). The introduction of doping ions could result in the formation of charged vacancies which may be attracted to the grain boundaries, thereby producing an excess concentration of doping ions near the grain boundary. Therefore, these adsorbed ions may serve as an impurity "atmosphere" which results in a substantial reduction in the grain boundary mobility.

Similar grain growth inhibition has been observed by Haertling (18) in a 2 atom percent bismuth ( $\text{Bi}^{+3}$ ) doped PZT (65/35 atom ratio of Zr/Ti) system. The data was obtained under pressure-sintering conditions and thus is the most comparable study to the present one available in the literature. Although a  $t^{1/3}$  dependence for grain growth was observed by Haertling the influence of the densification process, chemical homogenization, and porosity of the specimens from which the data was ascertained renders any interpreta-

tion questionable, particularly for short times and low temperatures. However, the data obtained at higher temperatures and longer times, where the above mentioned variables have probably been eliminated, does fit the cubic grain growth relationship and thus supports the solid solution (impurity) drag mechanism as proposed in the present study. Also, it is interesting to note that Haertling obtained a phenomenological activation energy of 95 K cal./mole for grain growth which is in reasonable agreement with the value (86 K cal./mole) determined in the present study.

Grain growth data obtained for heat treated specimens which experienced excessive PbO losses (>2.6 weight percent) were found to have grain sizes greater than what would be predicted by using the relation given in equation 5. A typical example would be a specimen which was heat treated for 11,400 minutes at 1200°C with a 3.53% weight loss. The specimen was determined to have a grain size of 8.2  $\mu\text{m}$  while the predicted value as determined from Fig. 6 would be approximately 5.6  $\mu\text{m}$ . These grain size differences between the experimentally observed values and the predicted values are considerably greater than any differences that might arise due to error in experimental technique. Thus, one is lead to believe that excessive PbO losses can rather drastically alter the grain growth rate of these materials.

Typical electron micrographs of polished and thermally etched specimens in order of ascending grain size are given in Figures 8-15. These micrographs portray the microstructural development



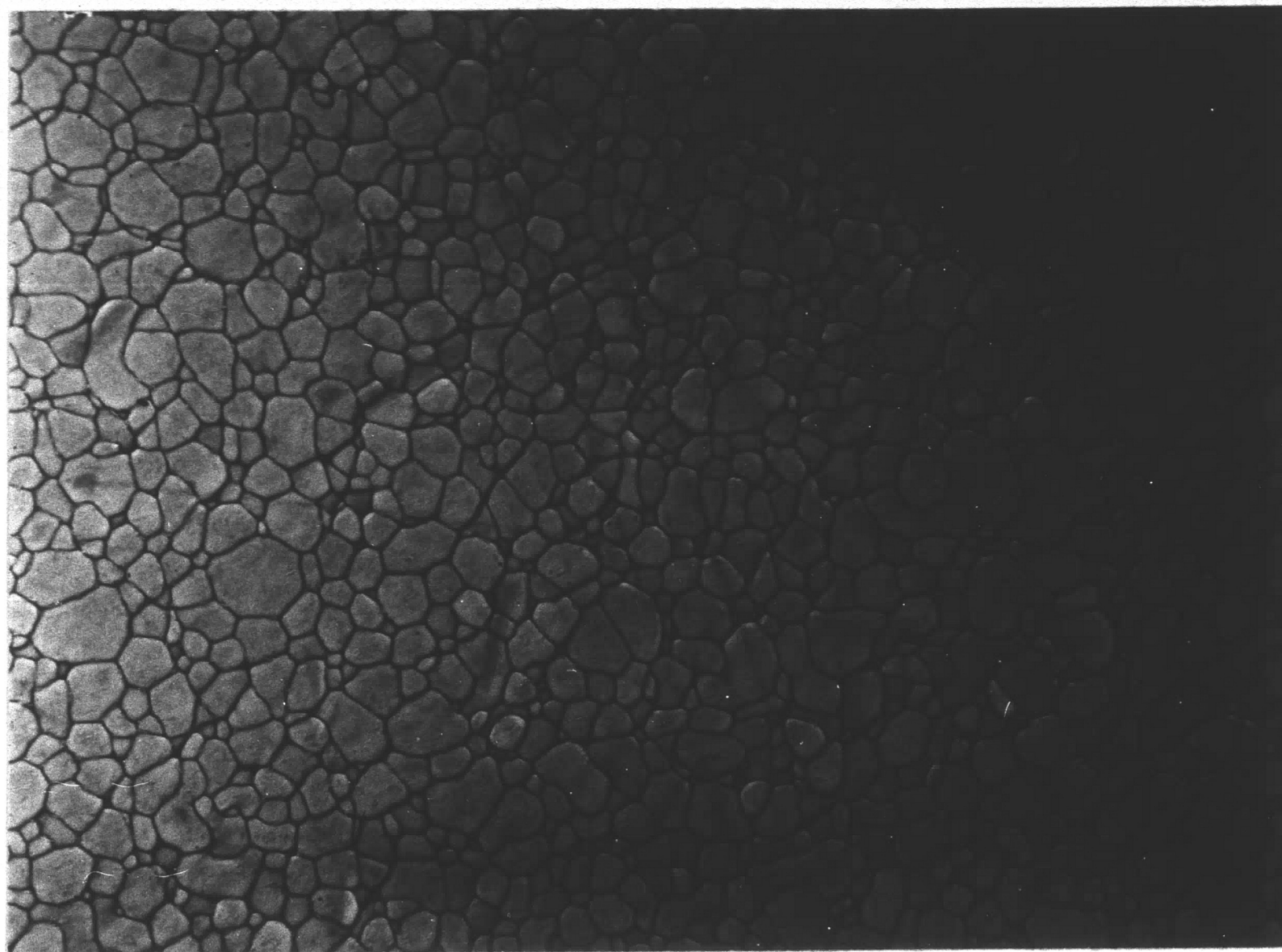


FIGURE 8  
ELECTRON MICROGRAPH SHOWING THE MICROSTRUCTURE OF  
PRESSURE-SINTERED PLZT (3,800X)

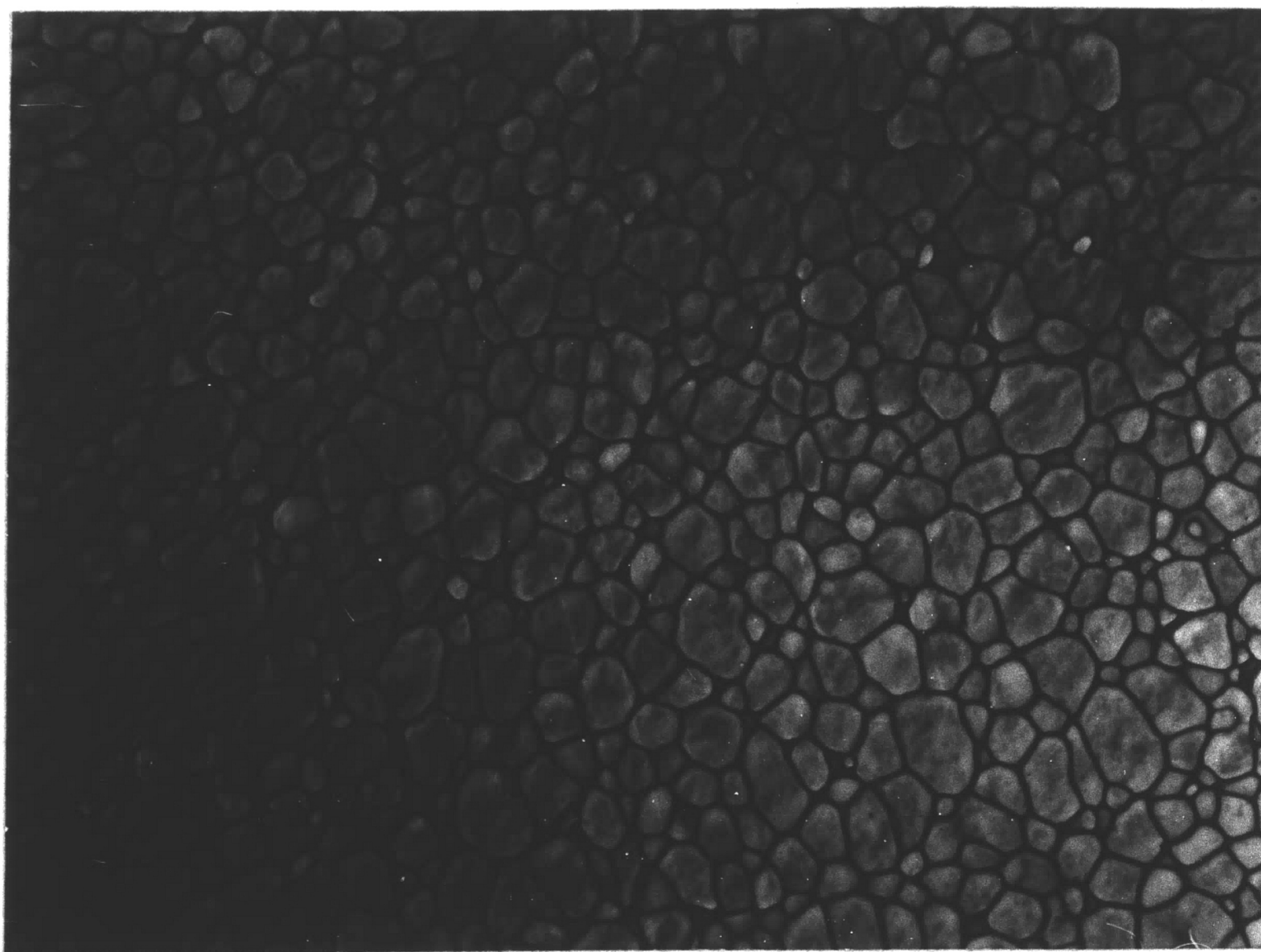


FIGURE 9  
ELECTRON MICROGRAPH SHOWING THE MICROSTRUCTURE OF  
PRESSURE-SINTERED PLZT (3,800X)



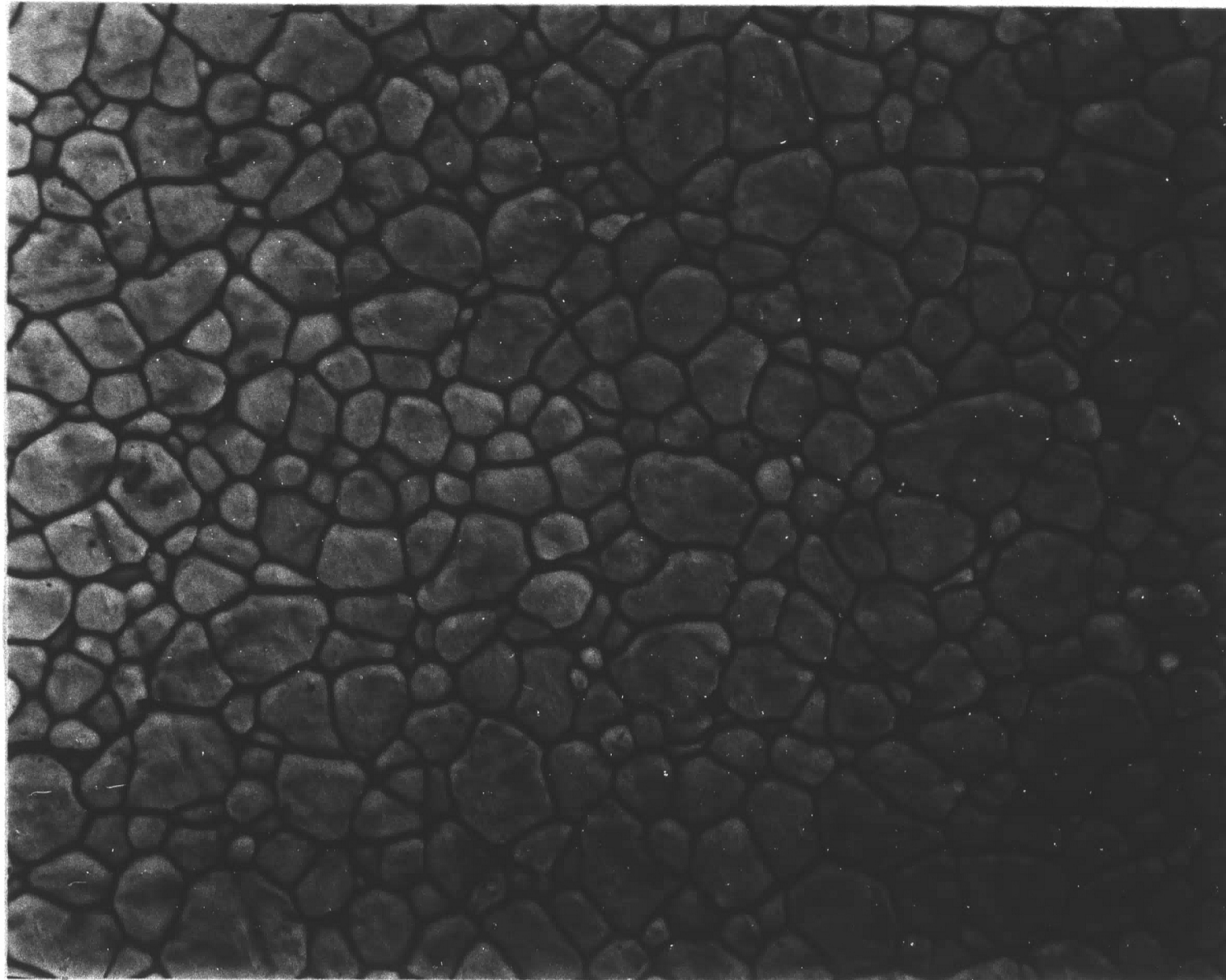


FIGURE 10

ELECTRON MICROGRAPH SHOWING THE MICROSTRUCTURE OF  
HEAT TREATED PLZT, 1100°C - 480 MINUTES (3,800X)

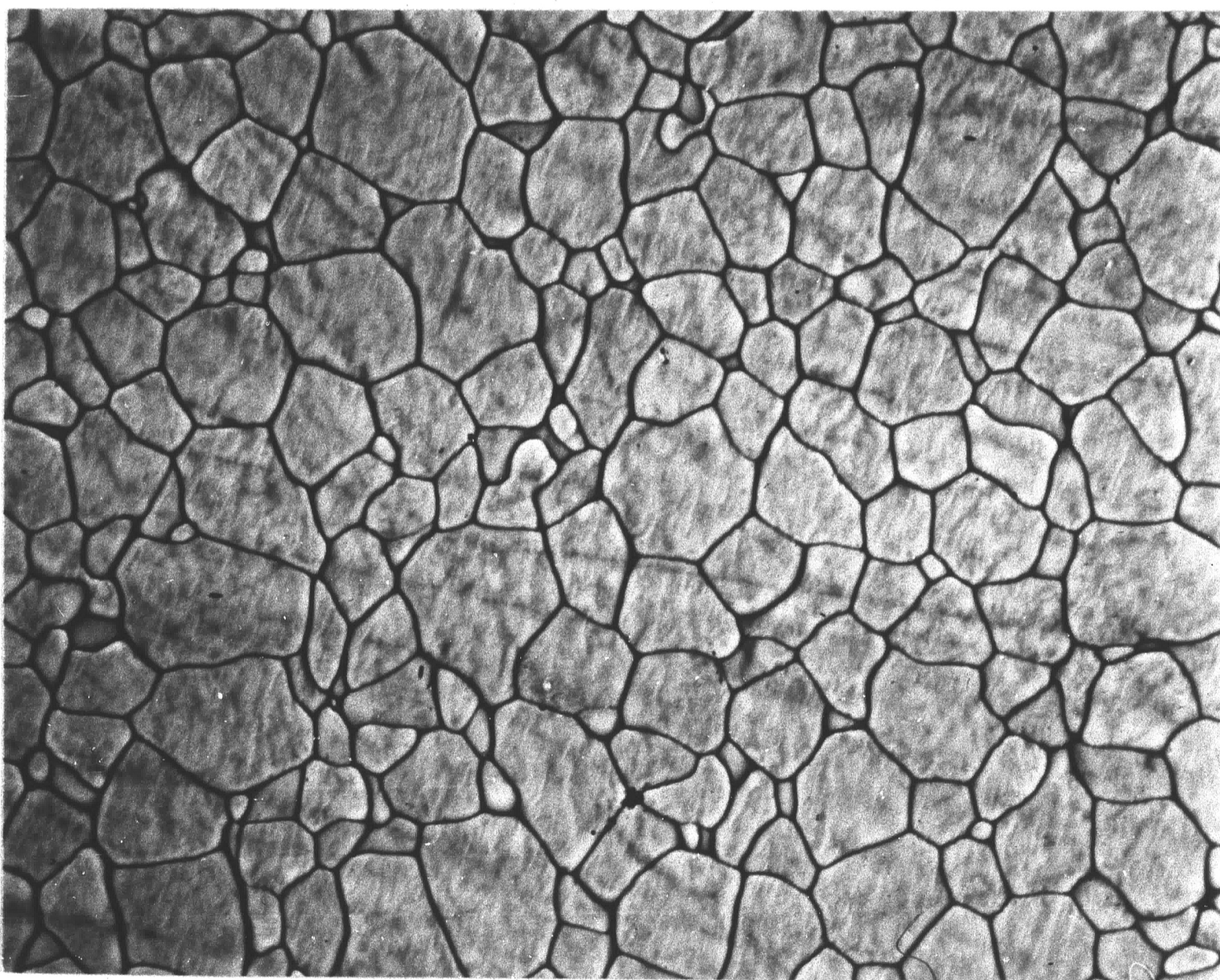


FIGURE 11

ELECTRON MICROGRAPH SHOWING THE MICROSTRUCTURE OF  
HEAT TREATED PLZT, 1100°C - 1,920 MINUTES (3,800X)



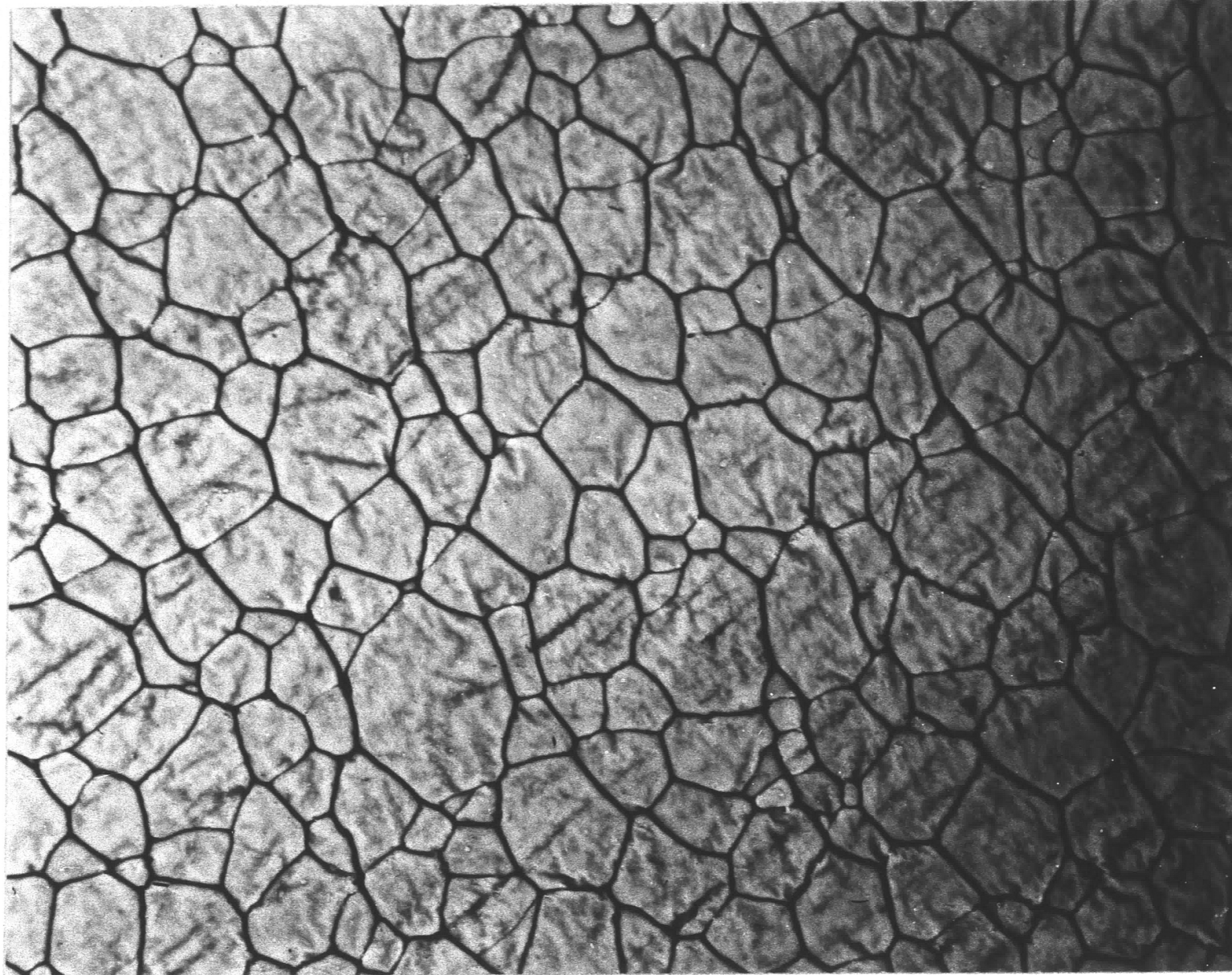


FIGURE 12

ELECTRON MICROGRAPH SHOWING THE MICROSTRUCTURE OF  
HEAT TREATED PLZT, 1200°C - 480 MINUTES (3,800X)

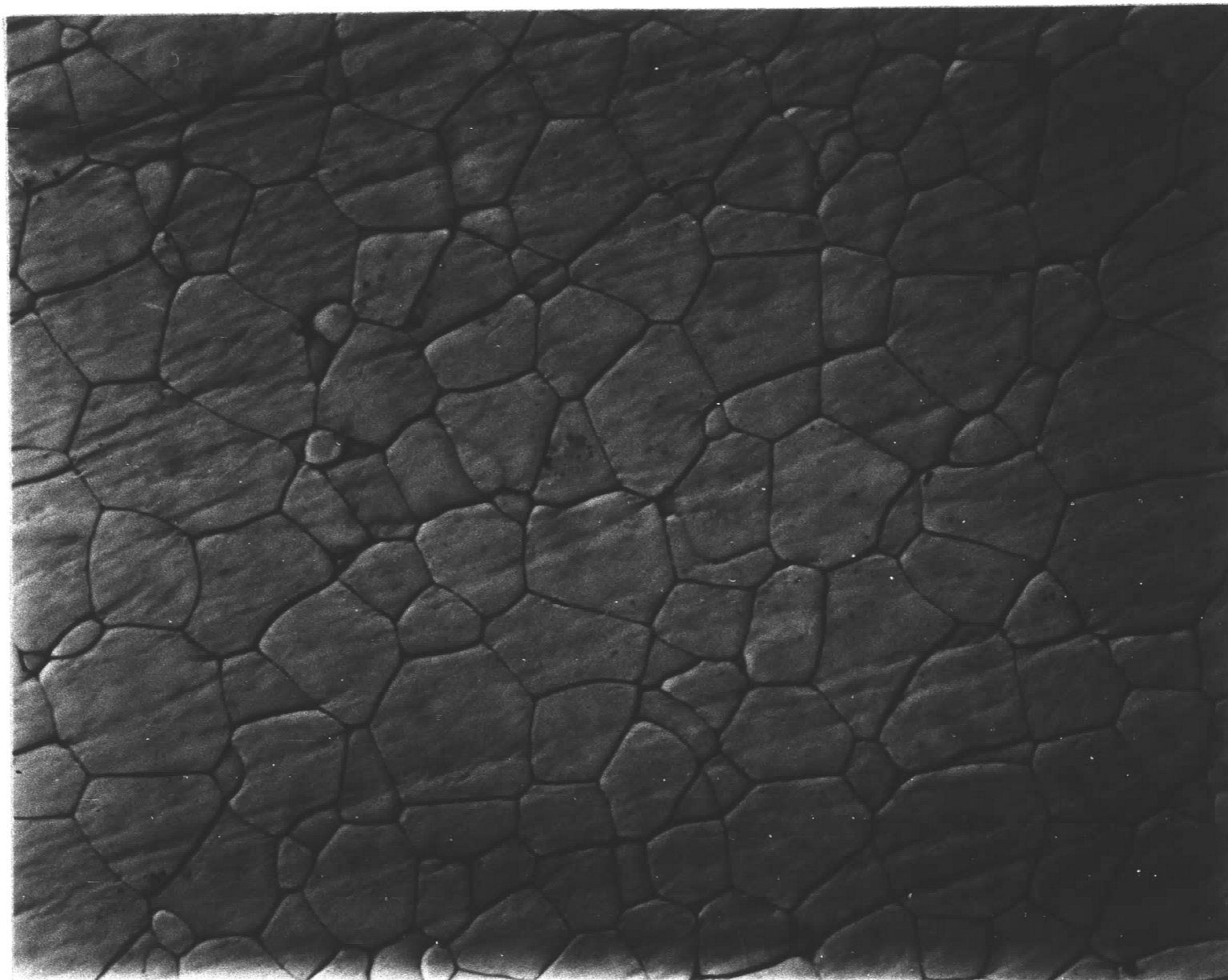


FIGURE 13

ELECTRON MICROGRAPH SHOWING THE MICROSTRUCTURE OF  
HEAT TREATED PLZT, 1100°C - 6,000 MINUTES (3,800X)



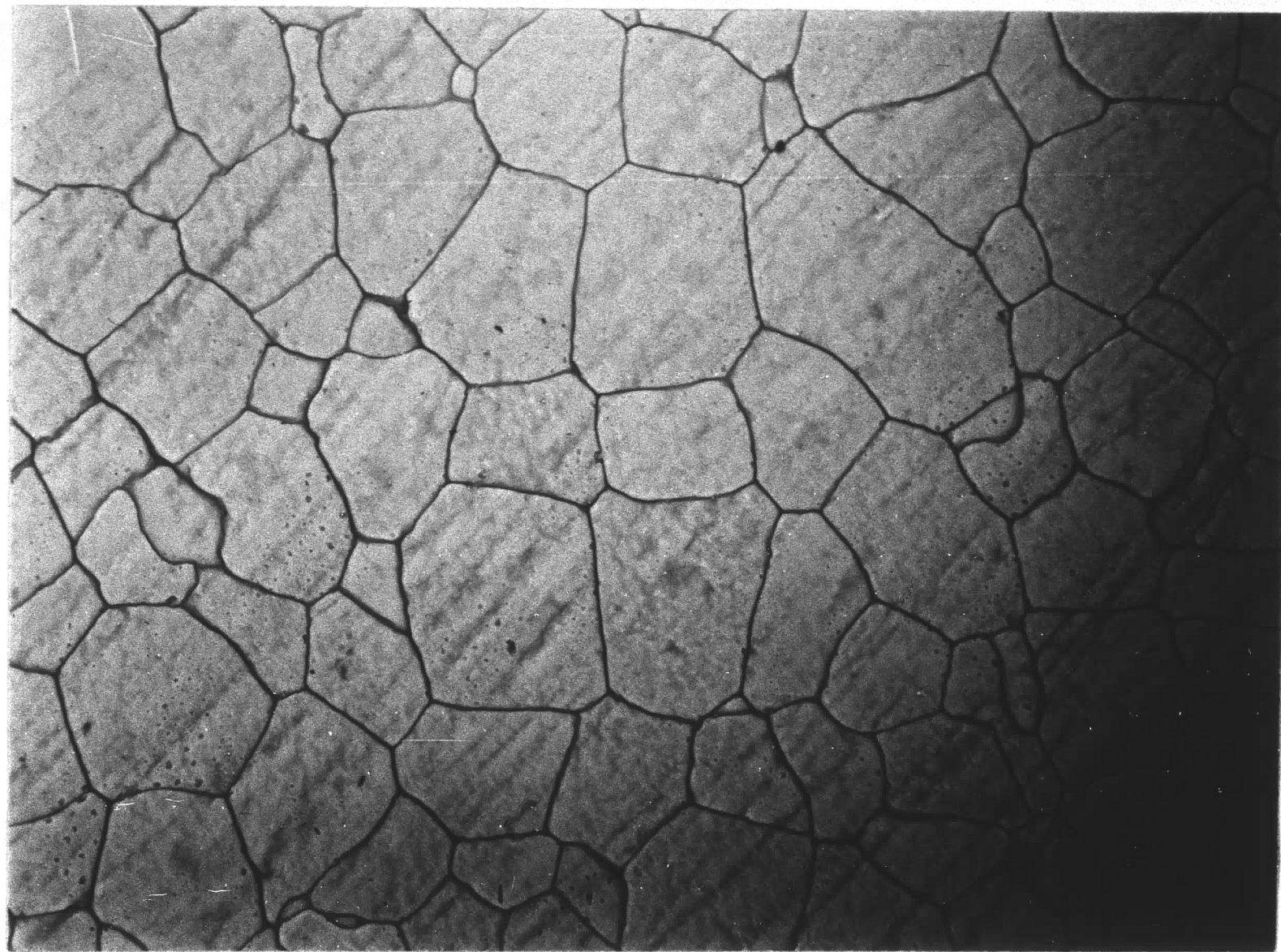


FIGURE 14

ELECTRON MICROGRAPH SHOWING THE MICROSTRUCTURE OF  
HEAT TREATED PLZT, 1200°C - 1.920 MINUTES (3,800X)

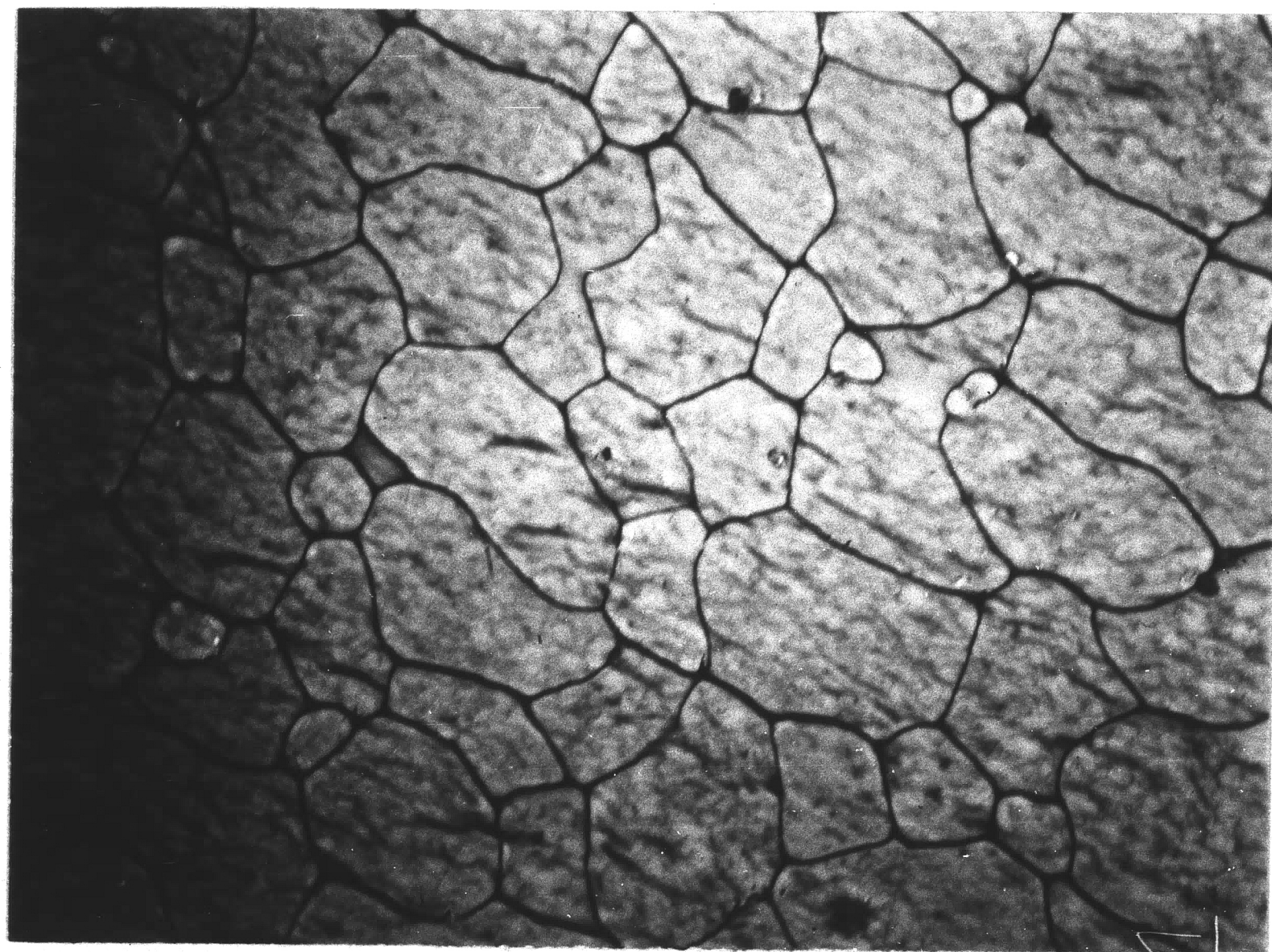


FIGURE 15

ELECTRON MICROGRAPH SHOWING THE MICROSTRUCTURE OF  
HEAT TREATED PLZT, 1200°C - 6,000 MINUTES (3,800X)



observed to take place during heat treatment. Scanning electron micrographs of a typical heat treated specimen which has been polished and one which has been polished and thermally etched is given in Figures 16-18. The presence of artifacts and polishing scratches can be observed in the micrographs, but they indeed substantiate the microstructural features revealed by the replica technique. In general, all the micrographs clearly illustrate that the heat treated specimens retain the basic microstructural characteristics of the initial pressure-sintered material, i.e., no exaggerated grain growth.

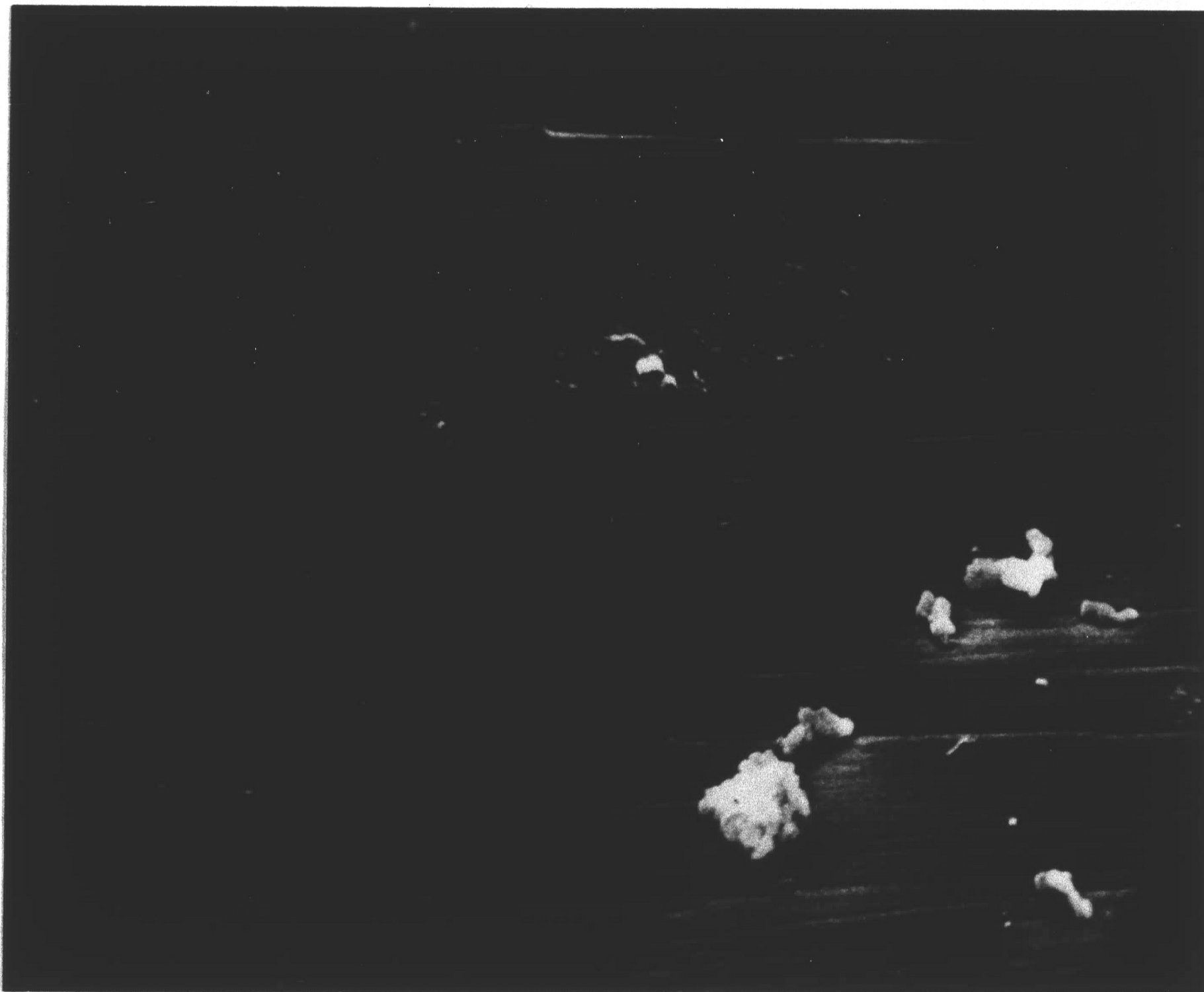


FIGURE 16

SCANNING ELECTRON MICROGRAPH OF A TYPICAL HEAT TREATED ( $1200^{\circ}\text{C}$ -  
4,320 MINUTES) SPECIMEN WHICH HAS BEEN POLISHED (5,250X)





FIGURE 17  
SCANNING ELECTRON MICROGRAPH SHOWING A TYPICAL HEAT TREATED SPECIMEN  
(1250°C-1,920 MINUTES) WHICH HAS BEEN THERMALLY ETCHED (2,100X)

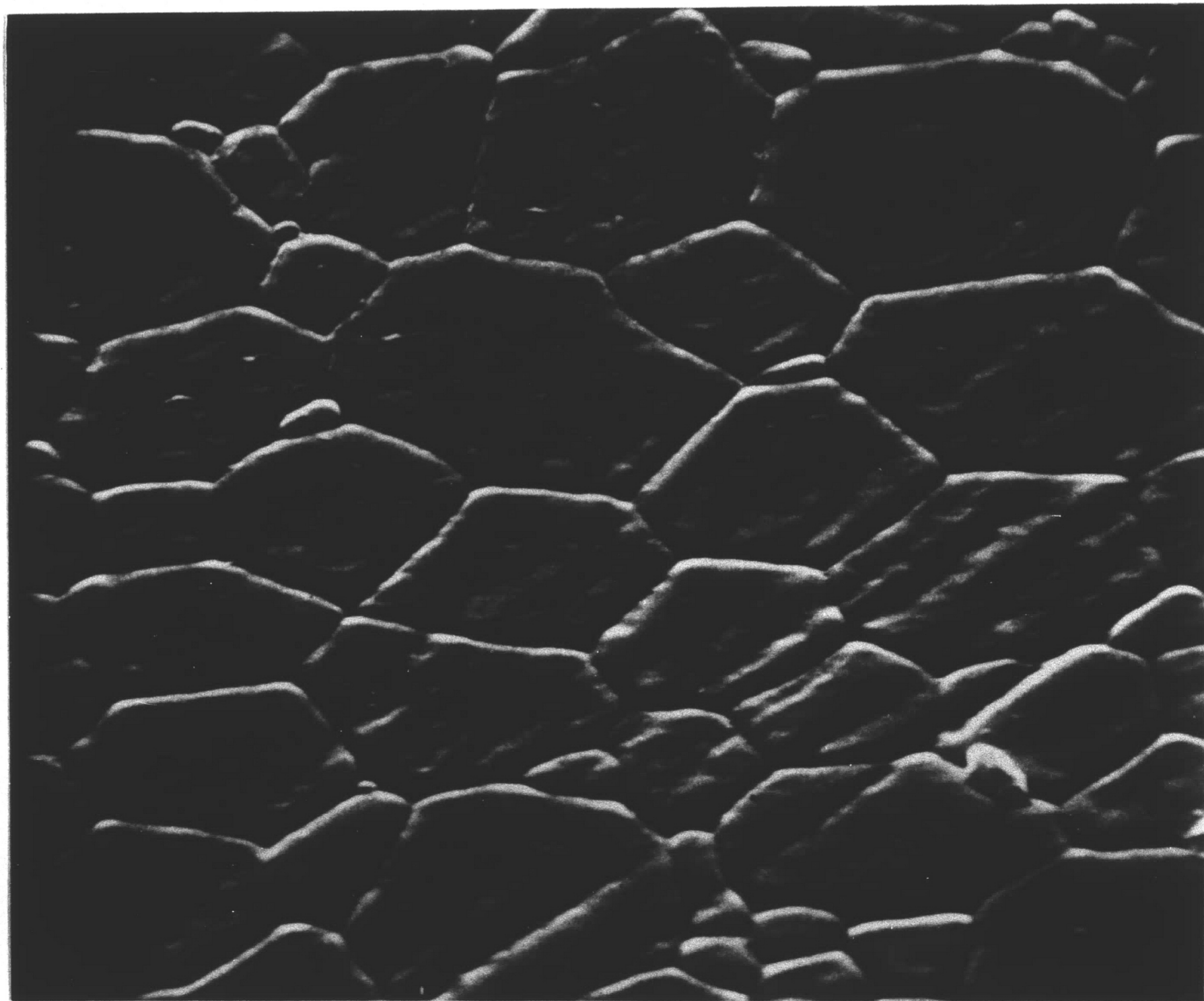


FIGURE 18  
SCANNING ELECTRON MICROGRAPH SHOWING A TYPICAL HEAT TREATED SPECIMEN  
(1250°C-1,920 MINUTES) WHICH HAS BEEN THERMALLY ETCHED (5,250X)



#### 4. Electrical and Electromechanical Properties

The effect of microstructure on the physical properties was investigated by isothermally heat treating fully dense specimens as discussed previously in sections II-4 and III-2. The specimens utilized in this investigation were heat treated at 1100°C, 1200°C, and 1250°C, and experienced weight losses (see Table III) as a consequence of the equilibration process. In all instances the weight losses were less than 2.6 weight percent and thus these specimens were considered to be in the single-phase field as discussed previously in section III-2.

The initial pressure-sintered slugs utilized in this investigation had average grain diameters of  $1.1 \pm 0.1 \mu\text{m}$ . Property measurements were performed on the disks originating from both the end and the center of each slug. Evaluation of the poled properties within a given slug revealed that in every case the center disk displayed slightly higher values for  $k_p$  and  $K_3^T$ , and slightly lower values for the dissipation factor (D.F.) relative to the end disk. Typical property differentials between the center and end disks within a slug were 0.03 for  $k_p$ , 100 for  $K_3^T$ , and 0.0020 for the D.F. The maximum deviation observed in one slug was 0.06, 277, and 0.0040 for  $k_p$ ,  $K_3^T$ , and D.F. respectively. Table V gives the initial properties of all the pressure-sintered slugs utilized.

In order to insure that the observed properties of the pressure-sintered disks were not in some fashion altered by the influence of

TABLE V  
 INITIAL ELECTRICAL AND ELECTROMECHANICAL PROPERTIES  
 OF THE PRESSURE-SINTERED SLUGS

Property		Pressure-Sintered Specimens	
$k_p$		0.535	+ 0.045
$K_3^T$	Unpoled	2234	+ 146
	Poled	2120	+ 140
D.F. (tan $\delta$ )	Unpoled	0.0230	+ 0.0027
	Poled	0.0240	+ 0.0040

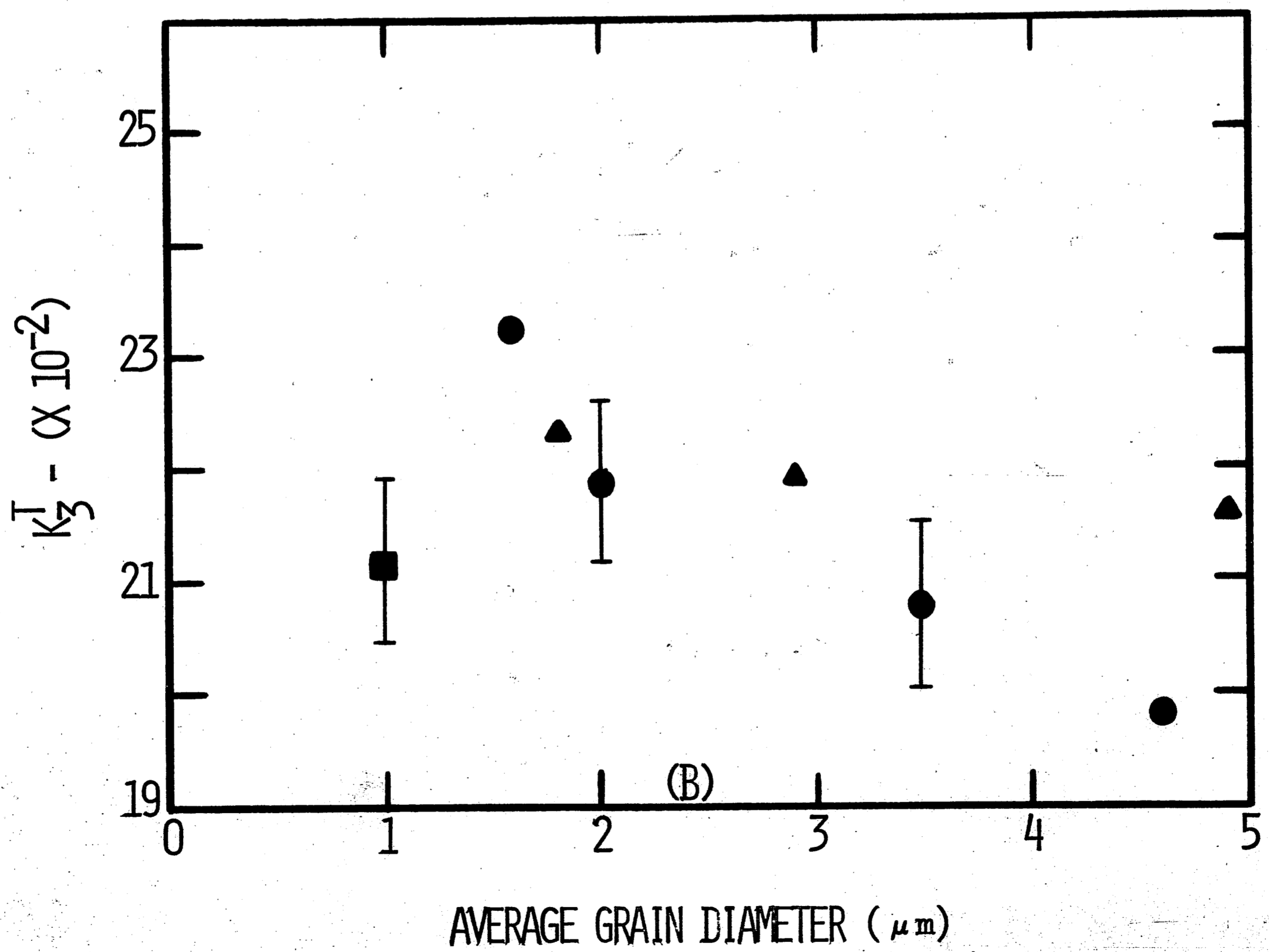
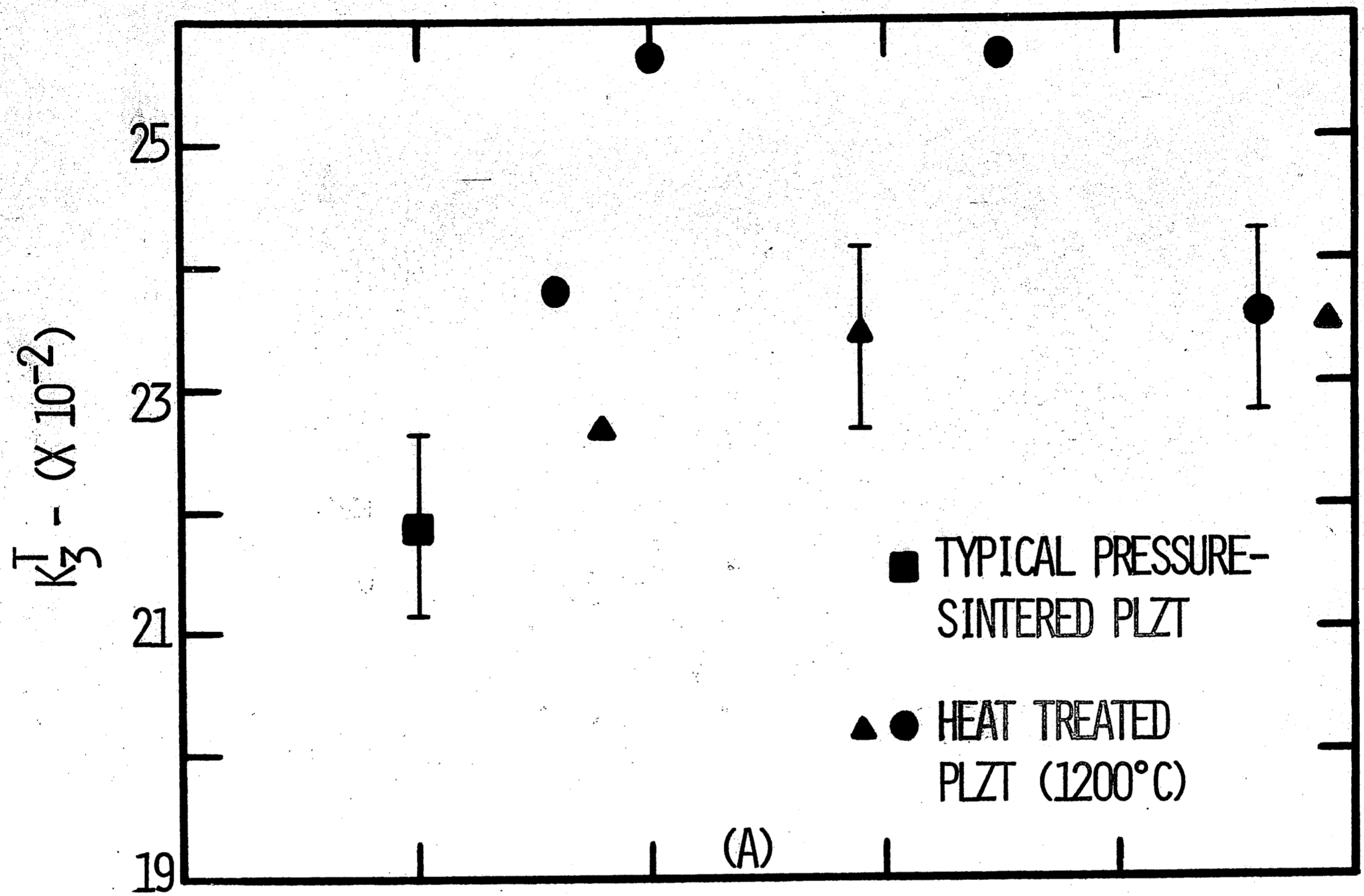


residual stresses due to the fabrication process, machining, etc. the samples were annealed. The annealing procedure consisted of taking the disks above their Curie temperature ( $\approx 150^{\circ}\text{C}$ ) and slowly cooling them. Upon re-evaluation of the properties 24 hours after poling it was generally observed that the annealing produced only slight property variations which were within the experimental error of the measurements.

It was found experimentally that when disks were selected randomly and heat treated, the resultant properties of these disks were not dependent upon the position of the disk within the original slug. For example, the slug which exhibited the greatest difference between the properties ( $\Delta k_p = 0.06$  and  $\Delta K_3^T = 277$ ) of center and end samples became very uniform ( $\Delta k_p = 0.01$  and  $\Delta K_3^T = 73$ ) upon heat treating at  $1200^{\circ}\text{C}$  for 480, 1920, and 6120 minutes.

The dielectric constant prior to poling is plotted in Fig. 19A as a function of the average grain diameter. In all instances it was observed that the dielectric constant of the unpoled pressure-sintered material was of a lower value than that of the heat treated specimens. No consistent variation of the unpoled dielectric constant with grain diameter was observed in this study. However, it has been commonly observed in PZT systems (19,29), with similar grain diameter ranges, that the dielectric constant decreases with increasing grain diameter. This effect in  $\text{BaTiO}_3$  has been explained by Buessum and co-workers (49) on the basis of

FIGURE 19  
DIELECTRIC CONSTANT ( $K_3^T$ ) UNPOLED (A) AND POLED (B)  
AS A FUNCTION OF AVERAGE GRAIN DIAMETER





internal stresses developed on passing through the Curie temperature. A larger grain diameter is thought to facilitate the reduction of stresses by the development of  $90^\circ$  domains within the grain, while a grain diameter approaching the size of the domains make this impossible.

On the basis of the experimental data in this work one would expect the domain size of the material to be relatively small compared to the grain size. Thus, an attempt was made to reveal the domain texture of the material and this is given in Fig. 20. Although the scanning electron micrograph does indeed confirm the presence of a fine domain texture further experimental studies should be conducted in order to conclusively establish the precise domain texture in PLZT materials.

The poled dielectric constant is plotted as a function of the average grain diameter in Fig. 19B. A slight trend towards lower dielectric constants with increasing grain diameter, for the heat treated specimens, is suggested. However, this effect is near the experimental error. Therefore, it was not considered useful to attribute this trend to a definite mechanism. Similar trends have been observed in PZT materials previously and explanations have been proposed (29).

The unpoled dissipation factor is plotted in Fig. 21A as a function of the average grain diameter. In all instances the heat treated specimens displayed higher values for the dissipation



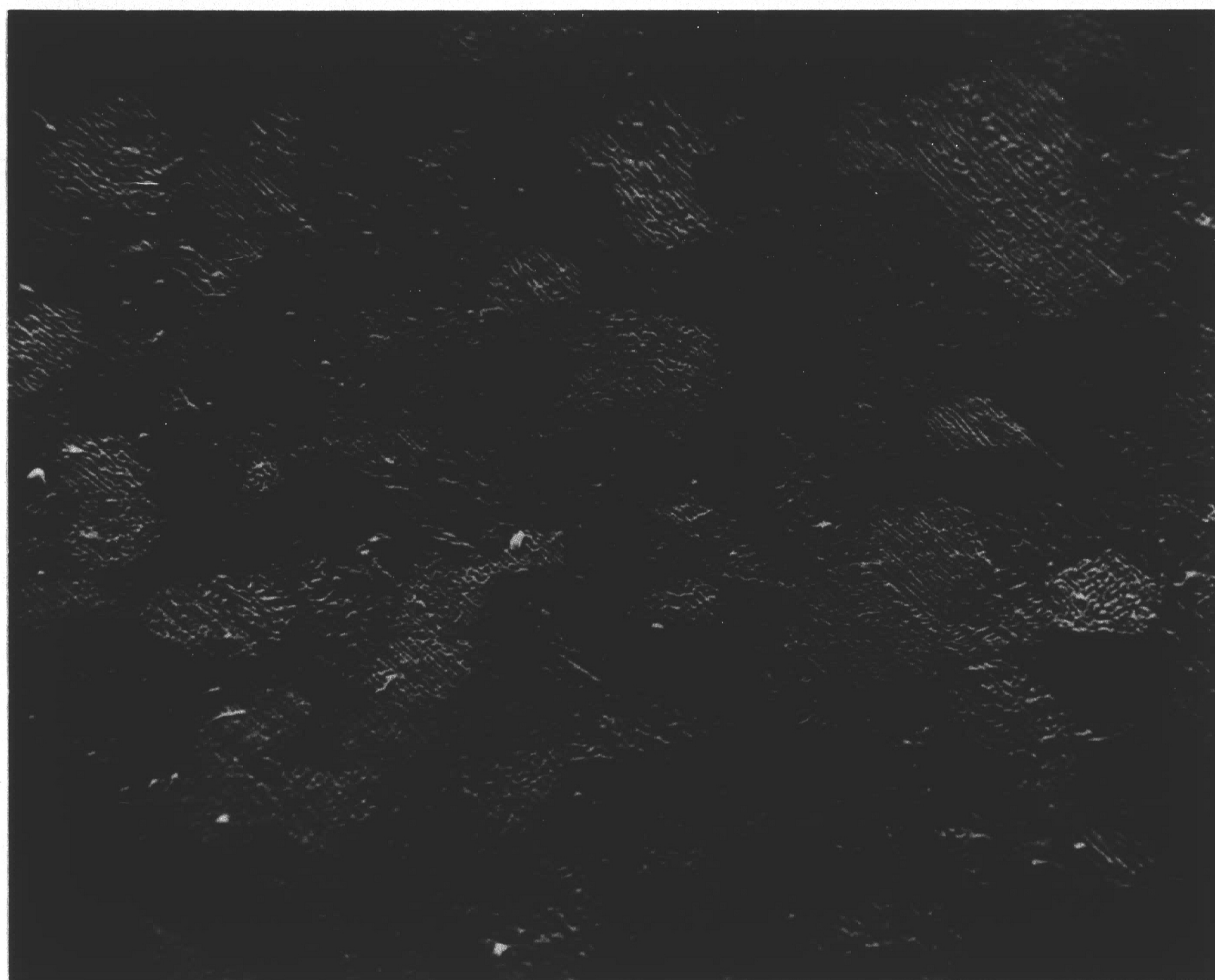


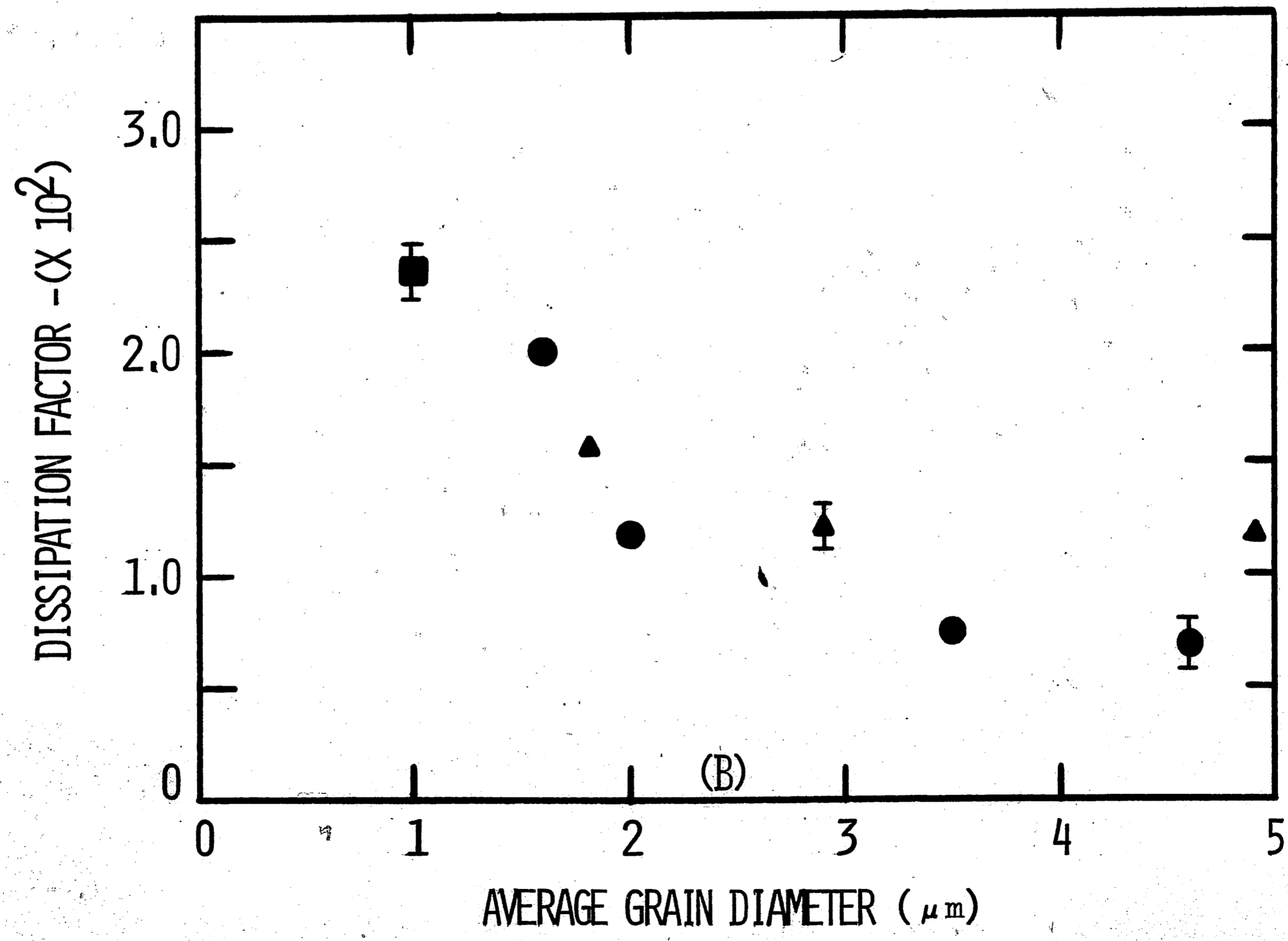
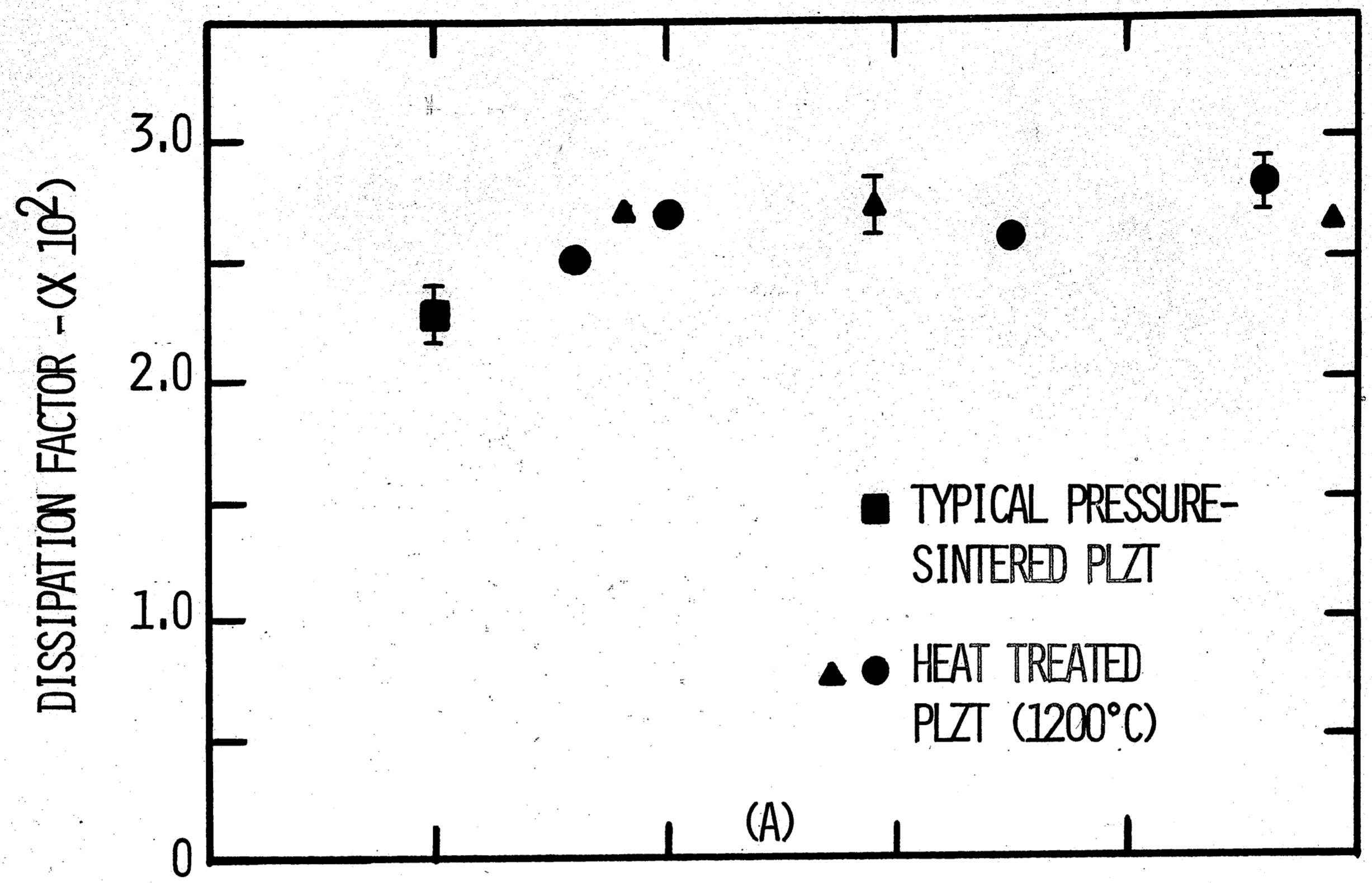
FIGURE 20

SCANNING ELECTRON MICROGRAPH SHOWING THE DOMAIN TEXTURE IN A  
TYPICAL HEAT TREATED (1200°C-4,320 MINUTES) SPECIMEN (2,100X)



FIGURE 21  
DISSIPATION FACTOR UNPOLED (A) AND POLED (B)  
AS A FUNCTION OF AVERAGE GRAIN DIAMETER





factor than that of the pressure-sintered specimens. No grain diameter effects upon the unpoled dissipation factor were in evidence.

The poled dissipation factor is plotted in Fig. 21B and property variation is observed to be dependent upon the average grain diameter. Similar grain diameter effects have been observed in PZT systems (6, 19, 29), but no conclusive explanations have thus far been proposed.

The planar coupling factor ( $k_p$ ) is plotted as a function of average grain diameter in Fig. 22. The coupling factor (which is proportional to the remanent polarization) increases with heat treatment, but is observed to become relatively constant with increasing grain diameter. In previous studies (20, 29) it has been observed that domain re-orientation in fine-grained material is inhibited and thus leads to a lower remanent polarization. This effect is not observed to be present in the heat treated specimens with grain sizes ranging from 1.5  $\mu\text{m}$  to 4.9  $\mu\text{m}$ . However, a significant increase in the planar coupling factor of the pressure-sintered material is achieved in going from  $\approx 1 \mu\text{m}$  to 1.5  $\mu\text{m}$ . This may be attributable to grain diameter effects, although this is not very probable (see Fig. 20). The most probable mechanism producing this increase in the planar coupling factor is the simultaneous stoichiometry change taking place during heat treatment. This will be discussed later.

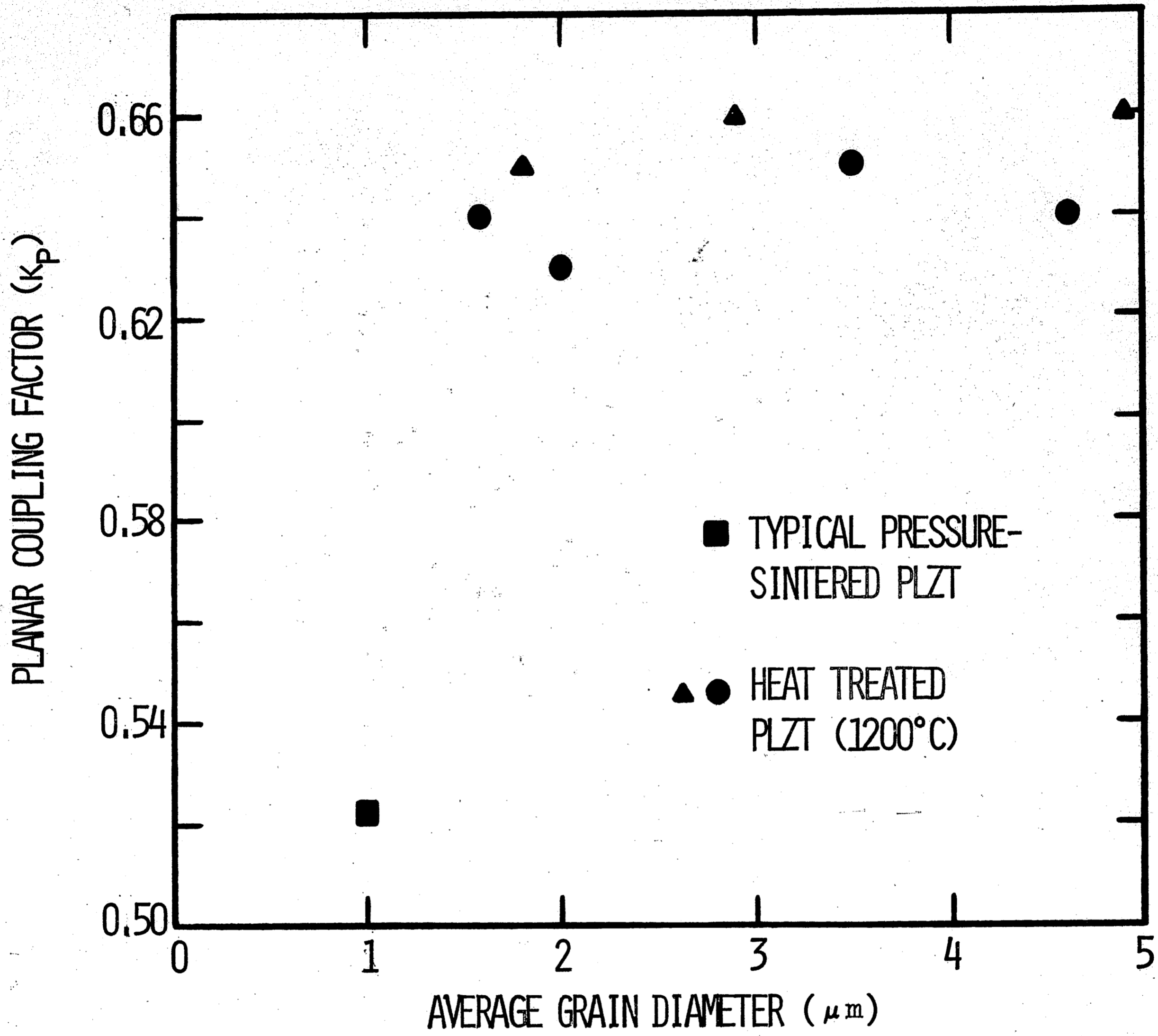


FIGURE 22  
PLANAR COUPLING FACTOR ( $k_p$ ) AS A FUNCTION OF  
AVERAGE GRAIN DIAMETER



The resonant frequency of the pressure-sintered material was observed to shift to lower frequency values upon heat treatment. This shift corresponds to a lowering of the mechanical stiffness of the pressure-sintered material. However, the resonant frequency was observed to be relatively constant in all the heat treated specimens and hence independent of the heat treatment temperature and grain diameter. The independence of the resonant frequency with grain diameter in fully dense materials has been previously established (50). It is therefore felt that the initial shift in the resonant frequency is not due to the increase in the grain diameter, but rather to an initial stoichiometry change (approximately  $\leq 1$  weight percent loss) experienced by the heat treated specimens.

The relative dielectric constant is plotted as a function of temperature in Figures 23 and 24 for specimens of various average grain diameters. The initial pressure-sintered material used in this study was observed to be comparable to the values reported in the literature by Haertling and Land (23). The relative dielectric constant reported for a 7/65/35 composition was approximately 12,000 at 150°C, this value is observed to be in excellent agreement with the data obtained in the present study. The effect of increasing grain diameter was to increase the relative dielectric constant at the Curie temperature. It is believed that this effect is due to the greater domain wall motion at low fields (1kHz) within the

FIGURE 23

DIELECTRIC CONSTANT AS A FUNCTION OF TEMPERATURE

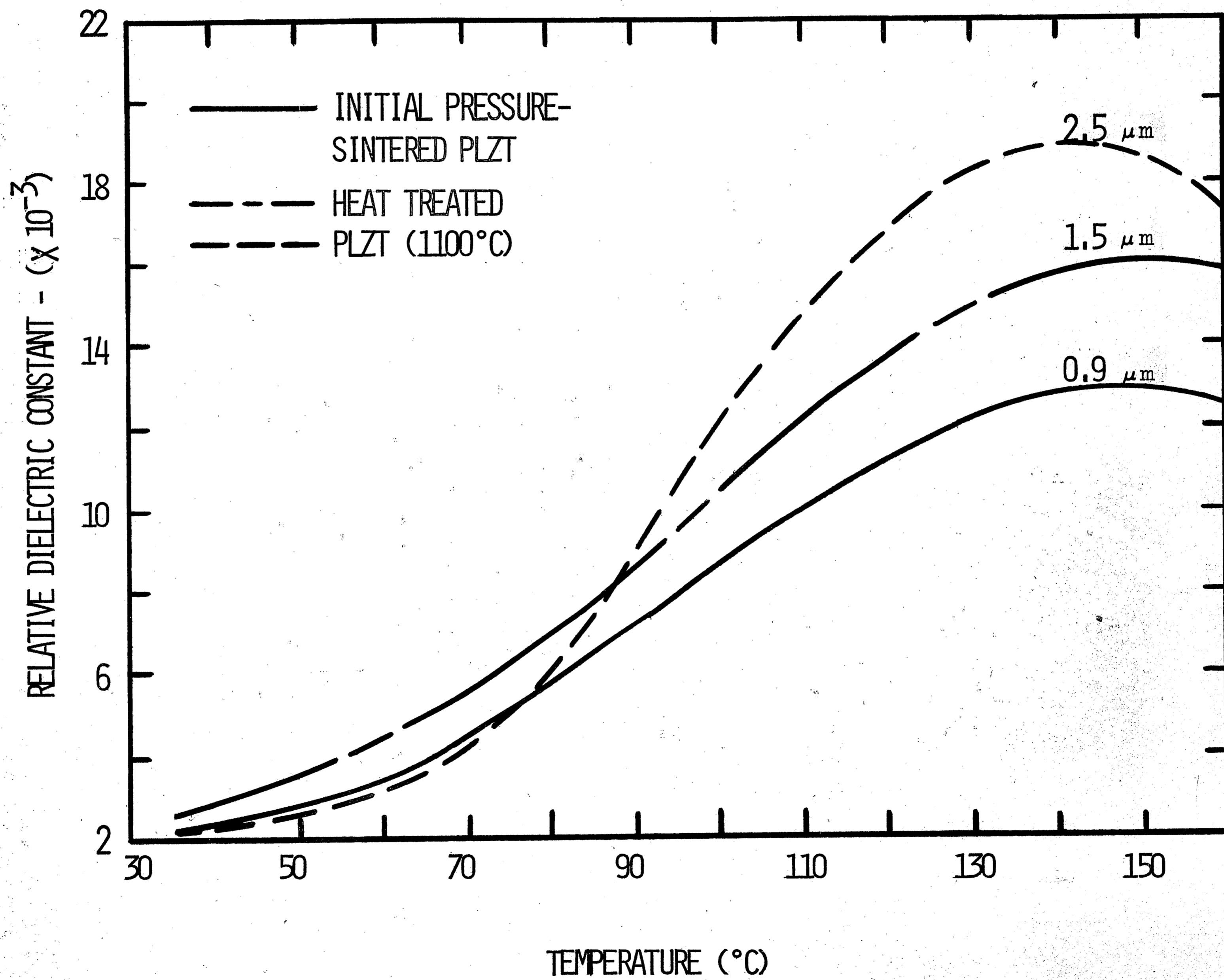
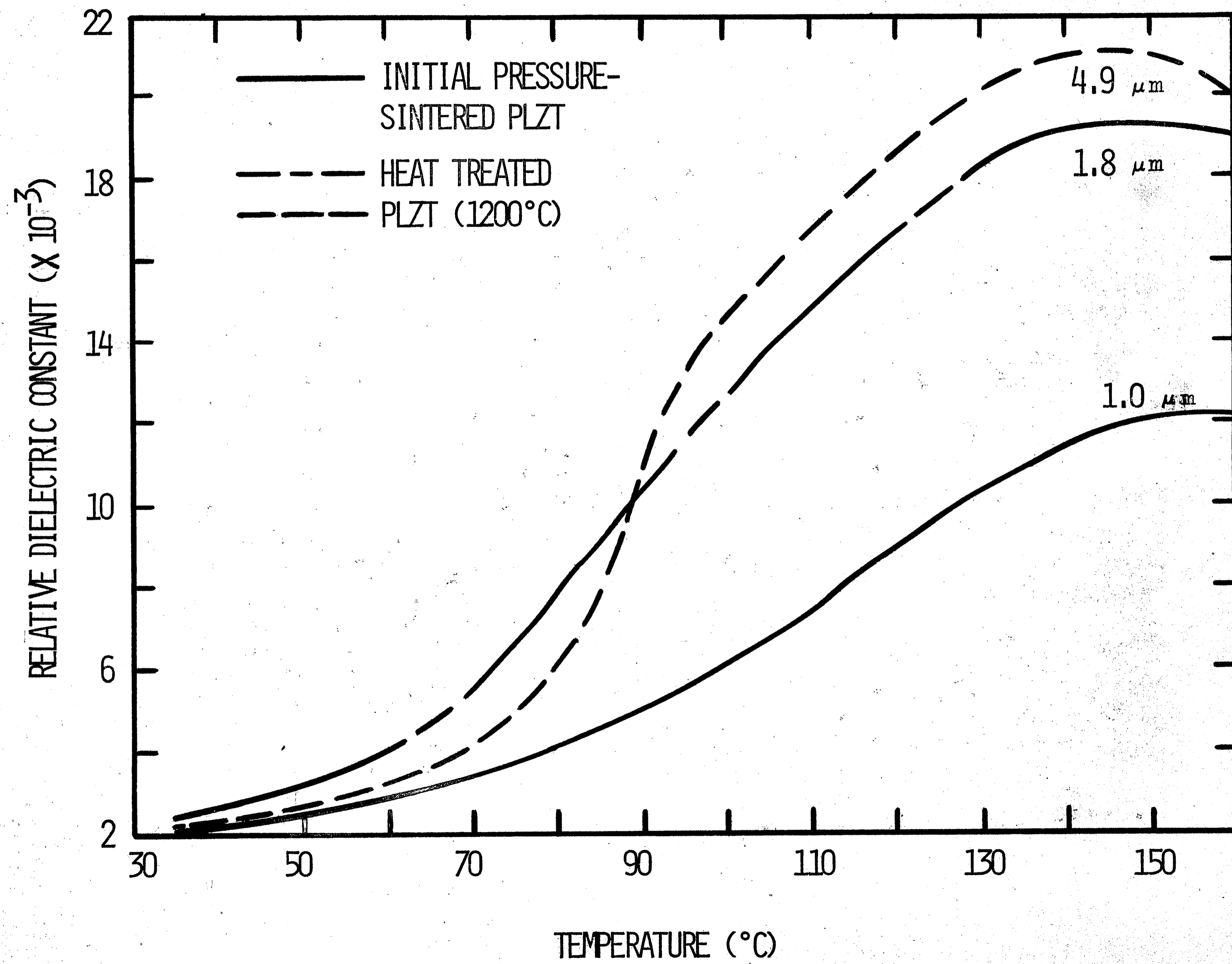




FIGURE 24  
DIELECTRIC CONSTANT AS A FUNCTION OF TEMPERATURE



large grain material.

Slight shifts in the relative dielectric constant peak towards lower ( $\approx 10^{\circ}\text{C}$ ) temperatures was observed in certain heat treated specimens given in Figures 23 and 24. The experimental procedure of monitoring the capacitance as a function of temperature used for this work was not well suited for the precise determination of the Curie temperature for PLZT materials. Therefore, further investigation of this trend towards lower Curie temperatures is necessary. The present data should be interpreted with care.

The values determined for the relative dielectric constant at the Curie temperature are plotted as a function of the average grain diameter in Fig. 25. The relative dielectric constant at the Curie temperature is dependent upon the specimens grain size and independent of the heat treatment temperature utilized to obtain this grain size. The curve drawn through the data points is only a visual estimate.

The dissipation factor was also measured as a function of temperature during the previously mentioned measurements. This data is plotted in Figures 26 and 27.

With respect to the observed property variation induced by the isothermal heat treatment, one must carefully consider all the possible mechanisms which may contribute to this variation. The three mechanisms thought to be of significant consequence to this study are: (1) the effect of grain size on the materials domain



FIGURE 25  
RELATIVE DIELECTRIC CONSTANT AT THE CURIE TEMPERATURE AS A  
FUNCTION OF AVERAGE GRAIN DIAMETER

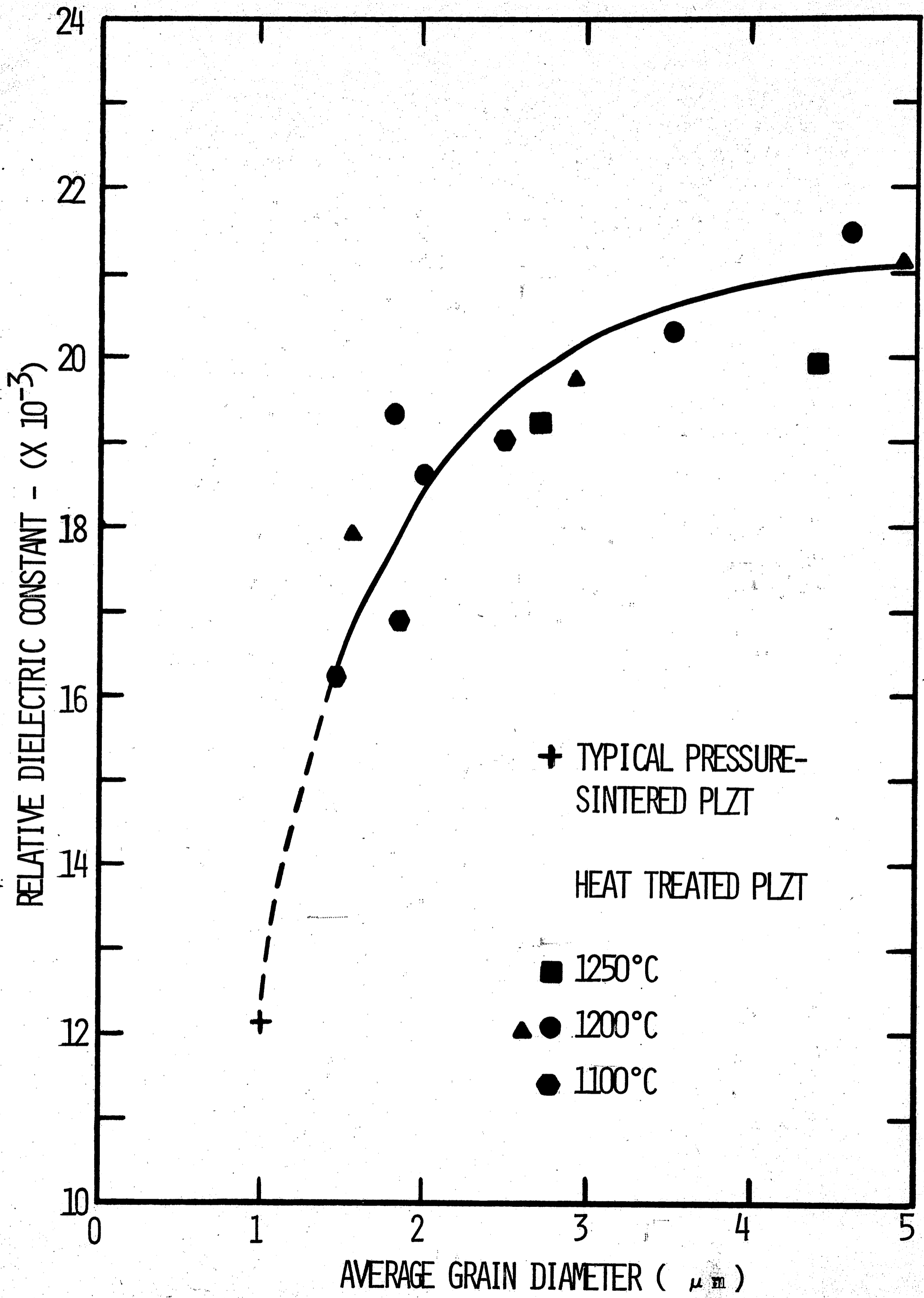


FIGURE 26  
DISSIPATION FACTOR AS A FUNCTION OF TEMPERATURE



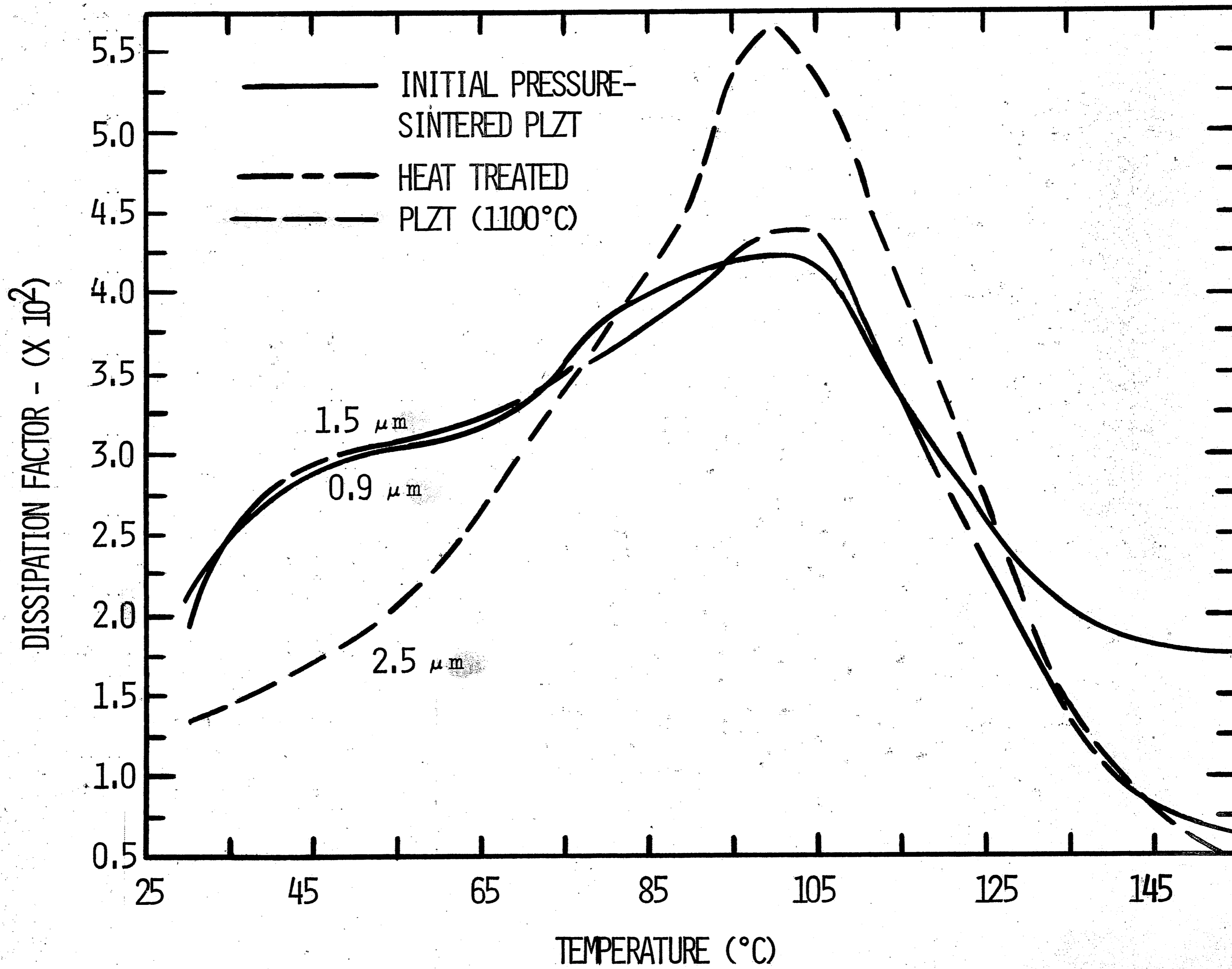
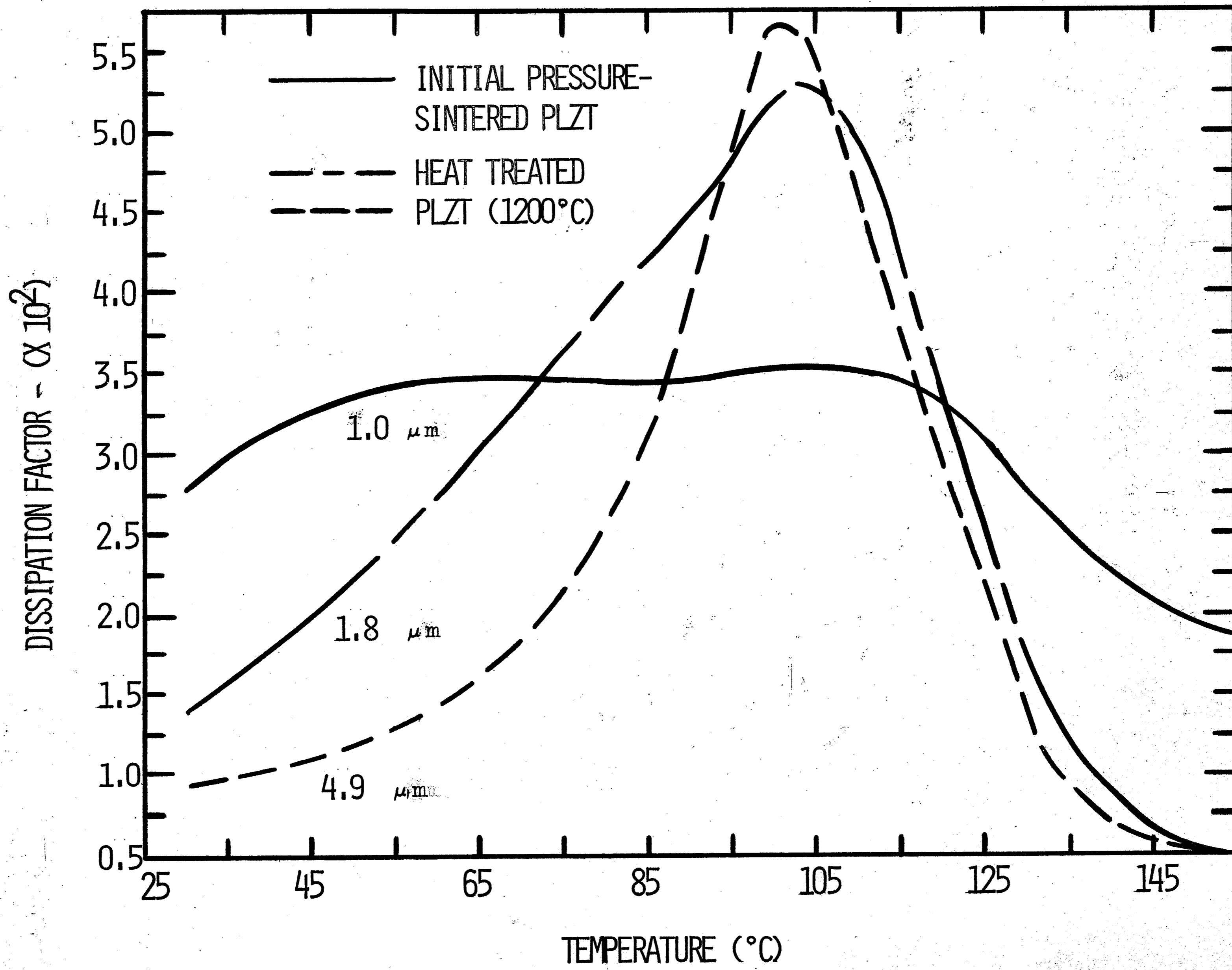


FIGURE 27  
DISSIPATION FACTOR AS A FUNCTION OF TEMPERATURE





texture, (2) the effect of stoichiometry changes (due to PbO losses during heat treatments) within the single-phase field on the domain wall motion, and (3) the loss of a sufficient amount of PbO to cause a compositional shift at high temperatures towards the rhombohedral-tetragonal phase boundary and the corresponding precipitation of a second phase. Of course any of the above may be occurring simultaneously.

The effect of grain diameter on a ferroelectric materials domain texture and domain wall mobility has been discussed previously in the text. Generally, these effects are related to the relative ease with which internal stresses can be relieved by a change in domain configuration. Therefore, property variation may be expected to occur if the domain size approaches the grain diameter making re-orientation of the domains difficult. This mechanism is probably not important here since the grain diameter appears to be much larger than the domain size.

The effect of stoichiometry variation due to the presence of Pb and O lattice vacancies on the ferroelectric behavior of doped and undoped PZT ceramics has been investigated (9, 51). In a similar PZT doped ( $\text{Bi}^{+3}$ ) system the remanent polarization was observed to increase upon rapid cooling from the sintering temperature and upon annealing in low Pb or O activity atmospheres. The observed increase in the remanent polarization of the bismuth doped PZT was attributed to an increase in the concentration of point

defects. Therefore, considering the experimental heat treating conditions employed in the present study, i.e. annealing in a low PbO activity atmosphere followed by a rapid quench, it is highly probable that the observed increase in  $k_p$  is facilitated by the introduction of point defects within the pressure-sintered material.

Property variations as a function of compositional change in the PLZT system has been investigated by Haertling and co-workers (23, 24). The PLZT phase diagram indicates that there are three possible paths by which a composition in the rhombohedral ferroelectric region can be modified such that it approaches the rhombohedral-tetragonal phase boundary. These three paths and the associated trends in property variation for a 7/65/35 PLZT composition are summarized in Table VI.

The experimental evidence of this work does not substantiate the mechanism by which property variation is achieved by means of a compositional shift towards the rhombohedral-tetragonal phase boundary. Since PbO loss during the equilibration process is the means by which a compositional shift would be accomplished, one would expect the properties to be dependent upon the amount of PbO lost by the specimen. Therefore, with increasing PbO loss, which corresponds to increasing isothermal heat treatment temperature, one would expect to observe increasing values for  $K_3^T$  and  $k_p$ . However, in the range measured this dependence of the properties was not observed. In general the determined values for  $K_3^T$  (poled

TABLE VI

Possible Paths By Which A Nominal 7/65/35 PLZT Composition  
 Can Approach The Rhombohedral-Tetragonal Phase Boundary And  
 The Effect of These Paths On Properties

<u>Property</u>	<u>Path 1*</u> <u>7 + X/65/35</u>	<u>Path 2*</u> <u>7/65 - Y/35 + Y</u>	<u>Path 3*</u> <u>7 + X/65 - Y/35 + Y</u>
$K_3^T$	Sharp Increase	Increase	Increase
$k_p$	Increase	Increase	Increase

\*Where X and Y are positive values



and unpoled), D.F. (poled and unpoled), and  $k_p$  were relatively constant (discounting grain size effects on the poled value of the D.F.) regardless of the heat treatment temperature providing further evidence of stoichiometry accommodation within the single-phase field.

On the basis of the experimental data obtained in this study and the findings previously cited in the literature it is thought that two mechanisms are responsible for the observed property variation. These two mechanisms are grain diameter effects and lattice vacancy effects. Grain diameter effects have been shown to be important as they relate to the poled dissipation factor and the dielectric constant at the Curie temperature.

The initial increase in the unpoled and poled dielectric constant, unpoled dissipation factor, and the planar coupling factor observed upon heat treating a pressure-sintered specimen, is thought to be dependent upon the initial stoichiometry change (approximately 1 weight percent loss). As expected the degree of stoichiometry change was observed to have little influence on the properties, since the difference in activities at the various temperatures is small (9) compared to the difference from the as-sintered samples. Therefore, there will be little property variation, as observed in the present study, between the specimens heat treated at various temperatures.

## IV. CONCLUSIONS

(1) Pressure-sintering conditions have been determined to produce theoretically dense PLZT specimens with average grain diameters of  $\approx 1 \mu\text{m}$ .

(2) Isothermal grain growth of fully dense, single-phase PLZT (7/65/35) in the presence of a low activity atmosphere (PbO) obeys the  $D^3 - D_0^3 = k' t$ , relationship. The mechanism controlling the grain growth rate is thought to be due to a solid solution (impurity) drag. The phenomenological activation energy for grain growth was calculated to be 86 K cal./mole.

(3) Grain diameter effects were observed to be important only as they relate to the poled dissipation factor and the relative dielectric constant at the Curie temperature. In the range studied ( $1 \mu\text{m} - 4.9 \mu\text{m}$ ) the dissipation factor was shown to decrease with increasing grain diameter, while the dielectric constant at the Curie temperature increased with increasing grain diameter.

(4) The isothermal heat treatment of pressure-sintered PLZT specimens, as performed in this study, increased the planar coupling factor approximately 20% in value, while the small signal dielectric measurements remained relatively constant (discounting grain diameter effects as mentioned above). This increase in the planar coupling factor is believed to be due to the introduction of point defects into the PLZT lattice.

(5) Single-phase PLZT exists over a range of stoichiometries corresponding to varying concentrations of lattice vacancies. Electrical and electromechanical properties were relatively insensitive to the degree of the stoichiometry change (as monitored by the sample weight loss) in the range measured (0.95% - 2.55%).



APPENDIX I

ELECTRICAL AND ELECTROMECHANICAL DATA

Heat Treating Temperature <sup>°C</sup>	Time (Minutes)	Grain Dia. (μ m)	%weight Change	Disk Number*	Prior to Poling		24 hours after poling		
					K <sub>3</sub> <sup>T</sup>	D.F.	K <sub>3</sub> <sup>T</sup>	D.F.	k <sub>p</sub>
-	0	0.9	0	1	2220	0.0207	2128	0.0245	0.55
-	0	0.9	0	5	2380	0.0226	2233	0.0225	0.58
1100	480	1.5	1.08	3	2521	0.0268	2420	0.0207	0.62
1100	1920	1.9	1.37	6	2510	0.0268	2387	0.0181	0.65
1100	6000	2.5	0.95	2	2389	0.0266	2090	0.0150	0.64
-	0	1.0	0	7	2119	0.0206	2075	0.0232	0.49
-	0	1.0	0	4	2180	0.0203	2150	0.0200	0.52
1200	180	1.6	1.62	2	2380	0.0250	2327	0.0200	0.64
1200	480	2.0	1.79	5	2569	0.0270	2186	0.0117	0.63
1200	1950	3.5	1.75	6	2570	0.0258	2076	0.0075	0.65
1200	6030	4.6	1.95	3	2361	0.0283	1983	0.0070	0.64
-	0	1.0	0	1	2088	0.0256	1980	0.0279	0.51
-	0	1.0	0	4	2347	0.0243	2257	0.0239	0.57
1200	480	1.8	1.71	2	2267	0.0271	2234	0.0157	0.65
1200	1920	2.9	1.94	3	2344	0.0274	2189	0.0123	0.66
1200	6120	4.9	1.80	5	2353	0.0265	2161	0.0120	0.66
-	0	1.1	0	1	2198	0.0251	2126	0.0260	0.52
-	0	1.1	0	4	2357	0.0243	2245	0.0255	0.55
1250	480	2.7	2.55	2	2409	0.0302	2223	0.0149	0.65
1250	1920	4.4	2.41	5	2511	0.0293	2144	0.0114	0.64

\*Disks numbered 3 and 4 originate from the approximate center of the pressure-sintered slug, while disks numbered 1 and 7 originate from the ends.

## REFERENCES

1. B. Jaffe, R. S. Roth, and S. Marzallo, "Properties of Piezoelectric Ceramics in the Solid-Solution series Lead Titanate - Lead Zirconate - Lead Oxide: Tin Oxide and Lead Titanate - Lead Hafnate," J. of Research of the National Bureau of Standards, 55 [5] 239-53 (1955).
2. R. Gerson, "Variation in Ferroelectric Characteristics of Lead Zirconate Titanate Ceramics Due to Minor Chemical Modifications," J. Appl. Phys., 31 [1] 188-94 (1960).
3. T. Skeda and T. Okano, "Piezoelectric Ceramics of  $Pb(Zr-Ti)O_3$  Modified by  $Al^{1+} B^{5+} O_3$  or  $A^{3+} B^{3+} O_3$ ," Jap. J. Appl. Phys., 3 [2] 63-71 (1964).
4. T. B. Weston, "Studies in the Preparation and Properties of Lead Zirconate - Lead Titanate Ceramics," J. Can. Ceram. Soc., 32 100-15 (1963).
5. N. Uchida and T. Ikeda, "Studies on  $Pb(Zr-Ti)O_3$  Ceramics with addition of  $Cr_2O_3$ ," Jap. J. Appl. Phys., 6 [11] 1292-99 (1967).
6. T. B. Weston, A. H. Webster and V. M. McNamara, "Lead Zirconate - Lead Titanate Piezoelectric Ceramics with Iron Oxide Additions," J. Am. Ceram. Soc., 52 [4] 253-57 (1969).
7. A. E. Crawford, "Lead Zirconate - Titanate Piezoelectric Ceramics," Brit. J. Appl. Phys., 12 529-34 (1961).
8. F. Kulcsar, "Electromechanical Properties of Lead Titanate Zirconate Ceramics Modified with certain Three- or Five-Valent Additions," J. Am. Ceram. Soc., 42 [7] 343-49 (1959).
9. R. B. Atkin and R. M. Fulrath, "Point Defects and Sintering of Lead Zirconate - Titanate," J. Am. Ceram. Soc., 54 [5] 265-70 (1971).
10. R. B. Atkin, R. L. Holman, and R. M. Fulrath, "Substitution of Bi and Nb Ions in Lead Zirconate - Titanate," J. Am. Ceram. Soc., 54 [2] 113-15 (1971).



## REFERENCES (cont)

11. J. Belding, "The Effects of High Electric Fields on Modified Lead Zirconate - Lead Titanate Ceramics for Piezoelectric Applications," Ph.D. Thesis, Rutgers-The State University, 1969.
12. T. B. Weston, A. H. Webster, and V. M. McNamara, "Variations in Properties with Composition in Lead Zirconate - Titanate Ceramics," J. Can. Ceram. Soc., 36 [15] 10-20 (1967).
13. A. H. Webster, T. B. Weston, and V. M. McNamara, "The Effects of Some Variations in Fabrication Procedure on the Properties of Lead Zirconate - Titanate Ceramics made from Spray-Dried, Co-precipitated Powders," J. Can. Ceram. Soc., 35 [61] (1966).
14. A. J. Mountvala, "Hot-Pressing Piezoelectric and Ferroelectric Materials," Am. Ceram. Soc. Bull., 42 [3] 120-21 (1963).
15. A. Kremheller and P. W. Renaut, "Ferroelectric Ceramics," Sylvania Technologist, 13 [3] 82-89 (1960).
16. P. D. Levett, "Factors Affecting Lead Zirconate - Lead Titanate Ceramics," Am. Ceram. Soc. Bull., 42 [6] 348-52 (1963).
17. G. H. Haertling, "Hot-Pressed Lead Zirconate - Titanate - Stannate Ceramics," Am. Ceram. Soc. Bull., 42 [11] 679-84 (1963).
18. G. H. Haertling, "Grain Growth and Densification of Hot-Pressed Lead Zirconate - Lead Titanate Ceramics Containing Bismuth," J. Am. Ceram. Soc., 49 [3] 118-18 (1966).
19. G. H. Haertling and W. J. Zimmer, "Analysis of Hot-Pressing Parameters for Lead Zirconate - Lead Titanate Ceramics Containing Two Atom Percent Bismuth," Am. Ceram. Soc. Bull., 45 [12] 1084-89 (1966).
20. G. H. Haertling, "Hot-Pressed Lead Zirconate - Lead Titanate Ceramics Containing Bismuth," J. Am. Ceram. Soc., 43 [12] 875-9 (1964).



## REFERENCES (cont)

21. G. H. Haertling, "Hot-Pressed Ferroelectric Lead Zirconate Titanate Ceramics for Electro-Optical Applications," *Am. Ceram. Soc. Bull.*, 49 [6] 564-67 (1970).
22. C. E. Land and P. D. Thacher, "Ferroelectric Ceramic Electrooptic Materials and Devices," *Proc. IEEE*, 57 [5] (1969).
23. G. H. Haertling and C. E. Land, "Hot-Pressed (Pb, La) (Zr, Ti)<sub>3</sub> Ferroelectric Ceramics for Electrooptic Applications," *J. Am. Ceram. Soc.*, 54 [1] 1-10 (1971).
24. G. H. Haertling, "Improved Hot-Pressed Electrooptic Ceramics in the (Pb, La) (Zr, Ti)<sub>3</sub> System," submitted to the *J. Am. Soc.*
25. J. R. Maldonado and A. H. Meitzler, "Ferroelectric Ceramic Light Gates Operated in a Voltage-Controlled Mode," *IEEE Trans. Elec. Devices*, 17 [2] 148-57 (1970).
26. P. D. Thacher and C. E. Land, "Ferroelectric Electrooptic Ceramics with Reduced Scattering," *IEEE Trans. Elec. Devices*, 16 [6] 515-21 (1969).
27. C. E. Land and R. Holland, "Electrooptic Effects in Ferroelectric Ceramics," *IEEE Spectr.*, 7 [2] 71-78 (1970).
28. A. H. Meitzler, J. R. Maldonado, and D. B. Fraser, "Image Storage and Display Devices Using Fine-Grain Ferroelectric Ceramics," *Bell Syst. Tech. J.*, 49 953 (1970).
29. A. H. Webster and T. B. Weston, "The Grain-Size Dependence of the Electromechanical Properties in Lead Zirconate - Titanate Ceramics," *J. Can. Ceram. Soc.*, 37 41-44 (1968).
30. E. C. Henry and A. V. Illyn, "Some Relationships between Grain Size and Properties in High-Purity Barium Titanate Ceramics," *J. Can. Ceram. Soc.*, 34 137-41 (1965).
31. R. Gerson and T. C. Marshall, "Dielectric Breakdown of Porous Ceramics," *J. Appl. Phys.*, 30 [11] (1959).

## REFERENCES (cont)

32. J. E. Hillard, "Estimating Grain Size by the Intercept Method," *Metal Progress*, 85 [5] 99-102 (1964).
33. R. L. Fullman, "Measurement of Particle Sizes in Opaque Bodies," *Trans. A. I. M. E.*, 197 [3] 447-52(1953).
34. IRE Standards on Piezoelectric Crystals: "Measurements of Piezoelectric Ceramics, 1961," *Proc. IRE (Inst. Radio Engrs.)* 49 [7] 1161-69 (1961).
35. D. A. Northrop, "Vaporization of Lead Zirconate - Lead Titanate Materials," *J. Am. Ceram. Soc.*, 50 [9] 441-45 (1967).
36. D. A. Northrop, "Vaporization of Lead Zirconate - Lead Titanate Materials: II, Hot-Pressed Compositions at Near Theoretical Density," *J. Am. Ceram. Soc.*, 51 [7] 357-361 (1968).
37. A. H. Webster, T. B. Weston and N. F. H. Bricht, "Effect of PbO Deficiency on the Piezoelectric Properties of Lead Zirconate - Titanate Ceramics," *J. Am. Ceram. Soc.*, 50 [9] 490-1 (1967).
38. J. E. Burke, "Grain Growth," in *Ceramic Microstructures*, edited by R. M. Fulrath and J. A. Pask, John Wiley and Sons, Inc., New York, (1968).
39. J. E. Burke and D. Turnbull, *Progress in Metal Physics*, vol. 3, edited by B. Chalmers, Pergamon Press, Oxford 1952.
40. F. A. Nichols, "Theory of Grain Growth in Porous Compacts," *J. Appl. Phys.*, 37 [13] 4599-602 (1966).
41. G. W. Greenwood, "The Growth of Dispersed Precipitates in Solutions," *Acta Met.*, 4 243-8 (1956).
42. W. D. Kingery and B. Francois, "Grain Growth in Porous Compacts," *J. Am. Ceram. Soc.*, 48 [10] 546-7 (1965).
43. R. J. Brook, "Pores and Grain Growth Kinetics," *Jour. Am. Ceram. Soc.*, 52 [6] 339-40 (1969).
44. M. Hillert, "On the Theory of Normal and Abnormal Grain Growth," *Acta Met.*, 13 227-38 (1965).



## REFERENCES (cont)

45. M. V. Speight, "Growth Kinetics of Grain - Boundary Precipitates," *Acta Met.*, 16 [1] 133-35 (1968).
46. K. W. Lay, "Grain Growth in  $UO_2 - Al_2O_3$  in the Presence of a Liquid Phase," *J. Am. Ceram. Soc.*, 51 [7] 373-76 (1968).
47. R. J. Brook, "Impurity Drag Effect and Grain Growth Kinetics," *Scripta Met.*, 2 [7] 355-78 (1968).
48. B. Jaffe, "Ferroelectric and Piezoelectric Properties," in *Ceramic Microstructures*, edited by R. M. Fulrath and J. A. Pask, John Wiley and Sons, Inc., New York, (1968).
49. W. R. Buessum, L. E. Cross and A. K. Goswami, "Phenomenological Theory of High Permittivity in Fine-Grained Barium Titanate," *J. Am. Ceram. Soc.*, 49 [1] 33-36 (1966).
50. J. B. Wachtman, Jr., "Mechanical Properties of Ceramics: An Introductory Survey," *Am. Ceram. Soc. Bull.*, 46 756 (1967).
51. R. B. Atkin, "Sintering and Ferroelectric Properties of Lead Zirconate Titanate," Ph.D. Thesis, University of California, Berkeley, (1970).



## VITA

Richard Allan Langman was born September 15, 1946, in Bay Shore, New York, the first son of Vincent Frederick and Patricia May Langman. Bred in nearby Massapequa, New York, he attended Massapequa High School graduating in 1964. The next four years were spent at Alfred University, Alfred, New York, in quest of a Bachelor of Science degree in Ceramic Engineering.

Upon graduation in June of 1968, he accepted a position with the Western Electric Company at their Allentown Works. During the next two years he enjoyed various product engineering responsibilities, and also attended Lehigh University's graduate school. Then in July of 1970 he was assigned to the Lehigh Master's Program at the Western Electric Corporate Education Center.

The author is a member of the American Ceramic Society and Keramos, the national professional ceramic engineering fraternity.